Available online at www.sciencedirect.com
ScienceDirect
Icarus 184 (2006) 255–276
ICARUS
www.elsevier.com/locate/icarus

A high-resolution infrared spectral survey of Comet C/1999 H1 Lee

Neil Dello Russo [a,b,c,*], Michael J. Mumma [b], Michael A. DiSanti [d], Karen Magee-Sauer [e], Erika L. Gibb [f], Boncho P. Bonev [b,g], I.S. McLean [h], Li-Hong Xu [i]

[a] *Department of Physics, The Catholic University of America, Washington, DC 20064, USA*
[b] *Solar System Exploration Division, NASA Goddard Space Flight Center, Code 690, Greenbelt, MD 20771, USA*
[c] *The Johns Hopkins University Applied Physics Laboratory, Laurel, MD 20723-6099, USA*
[d] *Planetary Systems Laboratory, Solar System Exploration Division, NASA Goddard Space Flight Center, Code 693, Greenbelt, MD 20771, USA*
[e] *Department of Chemistry and Physics, Rowan University, Glassboro, NJ 08028, USA*
[f] *Department of Physics and Astronomy, University of Missouri–St. Louis, St. Louis, MO 63121, USA*
[g] *Ritter Astrophysical Research Center, Department of Physics and Astronomy, The University of Toledo, Toledo, OH 43606, USA*
[h] *Department of Physics and Astronomy, University of California, Los Angeles, Los Angeles, CA 90095-1562, USA*
[i] *Department of Physical Sciences, Centre for Laser, Atomic and Molecular Sciences, University of New Brunswick, Saint John, NB E2L 4L5, Canada*

Received 23 September 2005; revised 3 April 2006

Available online 3 July 2006

Abstract

We obtained high-resolution ($\lambda/\Delta\lambda \sim 25{,}000$) spectra of Comet C/1999 H1 (Lee) on UT 1999 August 19.6 and 21.6 using the cross-dispersed Near InfraRed SPECtrometer (NIRSPEC) at the Keck Observatory atop Mauna Kea, HI. Here we present spectra of Comet Lee between 2.874 and 3.701 μm (3479–2702 cm^{-1}) representing the most complete high-resolution infrared survey of a comet to date in this wavelength region. Using published line lists and laboratory spectra we have identified 444 of the 545 distinct emission features present in these spectra. We have tabulated the rest frequencies, assignments, relative intensities, and signal-to-noise ratios of all detected emissions. In addition to gaining insights into the chemistry of Comet Lee, this survey provides a valuable tool for planning future high-resolution infrared observations of comets and other astronomical targets, and for retrospective comparison to existing high-resolution infrared datasets.

Keywords: Comets; Infrared; Observations; Spectroscopy

1. Introduction

Comets are volatile-rich, relatively unaltered remnants from the birth of the Solar System, so knowledge of their composition and structure gives information on the formation and evolution of volatile material within our Planetary System. The volatile compositions of comet nuclei have generally been inferred from the spectral signatures of gases forming their comae. While molecular dissociation fragments have been studied for nearly one hundred years (cf. Swings et al., 1941), the determination of their native precursors is often difficult. For example, despite the presence of strong CN and C_2 emissions in cometary spectra, the identity and source (from ice or dust) of their native precursors is still uncertain and in fact may differ among comets (cf. Manfroid et al., 2005; Combi and Fink, 1997).

The ability to study molecules directly released from the comet nucleus (parent or native volatiles) was first demonstrated with the detection of CO in Comets West 1976 VI and Bradfield 1979 X (Feldman, 1983), although CO can also be produced in significant amounts as a dissociation fragment. Later, parent volatiles HCN (Despois et al., 1986; Schloerb et al., 1986) and H_2O (Mumma et al., 1986) were detected in Comet Halley. Close spacecraft encounters with Comet Halley also provided insights into the volatile content of the coma and the nucleus. Abundances of several parent volatiles were determined from data obtained from the neutral gas mass spectrometer (NMS) aboard Giotto (Eberhardt et al., 1987a; Eberhardt, 1999). A low spectral resolution infrared spectrom-

* Corresponding author. Fax: +1 (240) 228 8939.
E-mail address: neil.dello.russo@jhuapl.edu (N. Dello Russo).

0019-1035/$ – see front matter
doi:10.1016/j.icarus.2006.04.020

eter on the Vega 1 spacecraft (IKS), achieved detections of H_2O, CO_2, H_2CO, and possibly CO (Combes et al., 1986, 1988; Mumma and Reuter, 1989).

IKS also detected a broad unknown spectral signature in the 3.2–3.6 μm region attributed primarily to C–H stretching vibrations in one or more organic compounds (Combes et al., 1988). Greenberg and Hage (1990) suggested that fluffy organic (CHON) grains could be the source for this X–CH emission, however, subsequent studies of additional comets suggested that this feature was primarily the result of infrared fluorescence from volatile species, with CH_3OH being a major contributor (Hoban et al., 1991; Reuter, 1992; Davies et al., 1993; DiSanti et al., 1995; Bockelée-Morvan et al., 1995).

Despite a demonstrated contribution from CH_3OH, evidence suggested that other gas phase species (likely organic) contributed significantly to the X–CH emission. Isolating and quantifying the individual molecules contributing to the X–CH feature was impossible at the low spectral resolving power ($R \equiv \lambda/\Delta\lambda \sim 10^3$ or less) delivered by the spectrometers available at that time.

Since the apparition of Halley, improvements in instrumental capabilities have permitted the routine detection of an increasing number of parent volatiles especially at infrared and radio wavelengths (cf. Biver et al., 2002; Mumma et al., 2003; Bockelée-Morvan et al., 2004). Recently, more than two-dozen parent volatiles were detected in the exceptionally bright Comet C/1995 O1 Hale–Bopp (cf. Crovisier, 1998). At infrared wavelengths, ground-based studies can now be done with greater sensitivity and higher spectral resolving power. High-resolution ($\lambda/\Delta\lambda > 10^4$) infrared spectroscopy has enabled individual ro-vibrational lines from cometary molecules to be resolved and distinguished from telluric absorptions, other molecular emissions, and the continuum. This permits the diagnostic detection of multiple unblended molecular emissions, making it possible to identify species that cannot be resolved or detected with low-resolution spectral observations. The first high-resolution ground-based spectrometer to operate between 2 and 5 μm was CSHELL (Tokunaga et al., 1990; Greene et al., 1993), at the NASA Infrared Telescope Facility (IRTF).

Comets C/1996 B2 Hyakutake, and C/1995 O1 Hale–Bopp were the first bright comets observed with CSHELL. Detections of methane (CH_4), ethane (C_2H_6), and acetylene (C_2H_2) established the importance of these symmetric hydrocarbons in comets and the need for high-resolution infrared spectroscopy to detect them (Mumma et al., 1996; Brooke et al., 1996, 2003; Magee-Sauer et al., 1999, 2002a; Dello Russo et al., 2001, 2002a; Gibb et al., 2003). The strength of ro-vibrational emissions in these comets demonstrated that CH_4 and C_2H_6 contribute significantly to the X–CH feature in at least some comets; so determining their abundances is essential for interpreting low-resolution infrared spectral data near 3.3 μm. CSHELL has been a workhorse in the study of comets, enabling the acquisition of valuable data for more than ten years. However, each grating setting only encompasses about 2.3×10^{-3} times its central frequency (in cm^{-1}), or $\sim$7 cm^{-1} in the L-band region (near 3.3 μm). This makes CSHELL a powerful instrument for studies focused on a limited number of important regions in the infrared spectrum, but inefficient for more complete spectral surveys.

A major advance in ground-based infrared spectroscopy was made with the commissioning of the near-infrared spectrometer NIRSPEC at the Keck II 10-m telescope in 1999 (McLean et al., 1998). By cross-dispersing the echelle grating and using a larger-format detector array, NIRSPEC combined the high spectral resolution of CSHELL with the greater spectral coverage of low-resolution spectrometers. NIRSPEC is equipped with a 1024×1024 InSb detector array, allowing greater spectral coverage per order (by about a factor of four) compared to CSHELL. NIRSPEC enjoys a further advantage in spectral coverage by employing a low-dispersion grating perpendicular to its echelle grating, allowing multiple orders (six in the L-band) to be cross-dispersed along the array (Fig. 1). NIRSPEC thereby achieves $\sim$25 times greater spectral coverage per echelle/cross-disperser setting in the L-band compared with a CSHELL grating setting. In addition, spectra obtained with NIRSPEC at Keck II are a factor of 3–5 more sensitive than those obtained with CSHELL at the IRTF. This increased spectral coverage and sensitivity permits studies of fainter comets, deeper searches for trace volatiles, and more complete spectral surveys that were previously impossible (or at least impractical) with CSHELL.

This paper reports results from a high-resolution ($\lambda/\Delta\lambda \sim 25{,}000$) spectral survey of Comet C/1999 H1 Lee between 2.874 and 3.701 μm (3479–2702 cm^{-1}) obtained with NIRSPEC. This spectral region contains ro-vibrational transitions for many molecules that are critical for interpreting the overall volatile composition of comets. Results from a subset of the Comet Lee data have been published elsewhere (Mumma et al., 2001a; Gibb et al., 2003; Bonev et al., 2004; Dello Russo et al., 2005; DiSanti et al., in preparation). This study will focus on identifying emissions observed in this spectral region, including H_2O, C_2H_2, C_2H_6, CH_4, HCN, NH_3, CH_3OH, H_2CO, OH, and NH_2. In this work we identify 444 of the 545 distinct emission features present in these spectra on two dates. We present extracted spectral residuals and tabulate the rest frequencies, assignments, relative intensities, and signal-to-noise ratios of all detected emissions. These data can help in the interpretation L-band spectra of other comets, and they constitute a valuable tool for future infrared studies of comets and other objects of astrophysical interest.

2. Observations and data reduction

We observed Comet Lee in August 1999 using NIRSPEC at the Keck II Telescope (Table 1). On UT August 19, we obtained three grating/cross-disperser settings (KL_A, KL_B, and KL_C) in order to obtain an overall survey of the L-band. On UT August 21, deeper searches for key organic species were done using two grating/cross-disperser settings (KL_D and KL_E). The wavelength range covered by these settings in orders 21–26 is given in Table 2 and Fig. 2. The slit was oriented east–west on the sky for all of these observations.

At each grating/cross-disperser setting, comet spectra were acquired using sequences of four scans with an integration time

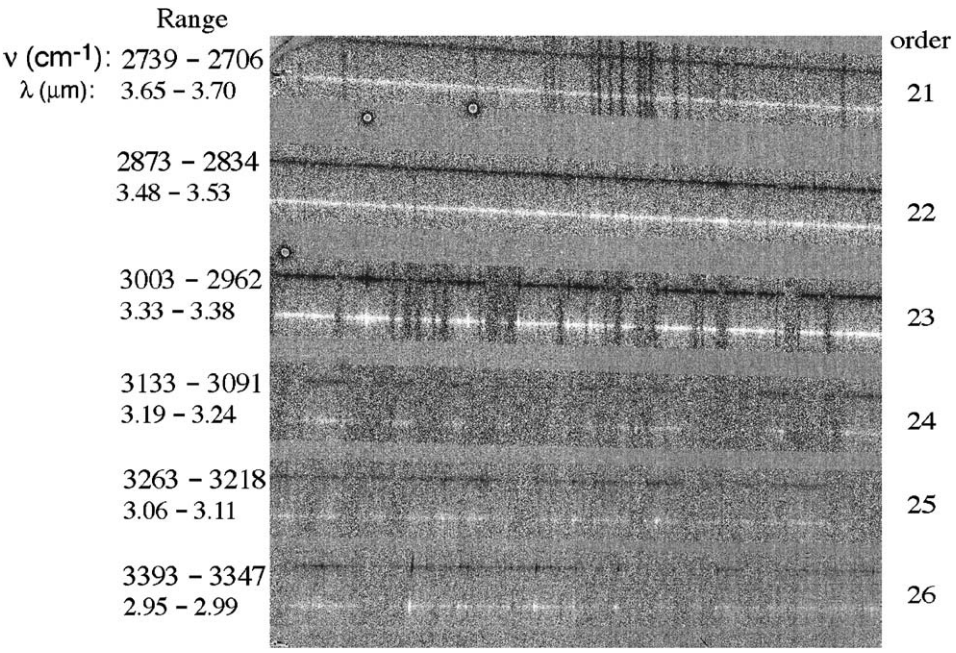

Fig. 1. A spectral difference (A–B) of Comet C/1999 H1 Lee obtained with NIRSPEC representing a single echelle/cross-disperser setting ($\lambda/\Delta\lambda \sim 25{,}000$). The telescope was nodded 12″ along the 24″ long slit, keeping the comet in the slit for both the A and B exposures. Each echelle/cross-disperser setting encompasses multiple orders (6 in this case) allowing an almost complete survey of the entire C–H stretch region with only three settings. In this study we are presenting spectra for 5 such settings between orders 21–26. Comet continuum and molecular line emissions are apparent in this raw spectral difference.

Table 1
Observing log for Comet C/1999 H1 Lee

UT date 1999[a]	R (AU)[a]	Δ (AU)[a]	Δ_{dot} (km s^{-1})[a]	$\lambda/\Delta\lambda$[ab]	Setting[c]	On-source time (min)
Aug. 19.6	1.049	1.381	−28.35	25,000	KL_A	8
					KL_B	8
					KL_C	10
Aug. 21.6	1.076	1.348	−29.03	25,000	KL_D	24
					KL_E	24

[a] R is the heliocentric distance, Δ is the geocentric distance, Δ_{dot} is the geocentric velocity, and $\lambda/\Delta\lambda$ is the spectral resolving power.

[b] High-dispersion spectra were acquired with a 3-pixel wide slit (0.43″ × 24″ on the sky).

[c] The spectral range of each setting is given in Table 2.

of 1 min on-source per scan (4 min for the total sequence). For all comet observations we used a slit length of 24″ (∼125 pixels) and a slit width of 0.43″ (3 pixels) on the sky. The telescope was nodded 12″ along slit such that the comet remained in the slit for both A- and B-beam integrations (Fig. 1). The observations were acquired in the sequence ABAB on UT Aug. 19, and in the sequence ABBA on UT Aug. 21.

Data processing included removal of cosmic ray hits and high dark current pixels. Taking a difference of A and B frames removes background sky and telescope emissions, revealing the comet emissions as tilted horizontal signatures at the A- (white) and B- (black) beam positions (Fig. 1). The tilted dark vertical features extending across an order are incompletely canceled sky emission lines (e.g., see order 21 in Fig. 1). Each order within a grating/cross-disperser setting was "clipped-out" and analyzed independently. We resample each order such that the spectral dimension falls along rows and the spatial dimension falls along columns (see, e.g., Fig. 2B in Mumma et al., 2001a).

We achieve spectral registration along slit and establish accurate wavelength calibration by use of the Spectrum Synthesis Program (SSP; Kunde and Maguire, 1974), which accesses the HITRAN-1992 molecular database (Rothman et al., 1992). We generate a fully-resolved synthetic spectrum of radiant sky emission, and a transmittance spectrum of the terrestrial atmosphere based on an initial estimate of the column burdens of absorbing molecules. The positions of sky lines in a radiance spectrum are matched to corresponding sky line emissions in an A (or B) frame at various positions along the slit, thereby converting the spectral dimension from pixels to wavenumbers and providing row-by-row spectral registration along the entire length of the slit. The calibration solution is applied to an extracted one-dimensional comet spectrum, which contains comet continuum and line emissions. The atmospheric transmittance model is optimized by matching the column burdens for atmospheric species to those in the observed comet spectrum. The optimized synthetic transmittance model is then binned to the instrumental sampling interval, convolved to the spectral resolution of the comet data, and scaled to the comet continuum. The synthetic transmittance model is scaled to continuum points in the comet spectrum that are chosen in regions of high atmospheric transmittance and also free of any apparent cometary molecular emission (see, e.g., Figs. 2c and 3 in Mumma et al., 2001a; see also Appendix 2 in Bonev, 2005, for a more detailed guide to NIRSPEC comet data reduction).

Volatile emission features were isolated from the continuum by subtracting the scaled atmospheric model from the comet spectrum, yielding the net observed molecular emissions (residuals)—these are still convolved with the atmospheric

Table 2
Spectral grasp of the NIRSPEC settings

Setting	Spectral grasp (cm^{-1})[a]					
	Order 26	Order 25	Order 24	Order 23	Order 22	Order 21
KL_A	3387–3347	3257–3216	3128–3085	2998–2957	2868–2830	2731–2702
KL_B	3478–3430	3347–3299	3216–3168	3084–3036	2951–2905	2813–2774
KL_C	3433–3384	3302–3255	3171–3125	3040–2995	2908–2866	2772–2736
KL_D	3393–3347	3263–3218	3133–3091	3003–2962	2873–2834	2739–2706
KL_E	3466–3413	3333–3283	3201–3152	3068–3022	2935–2891	2798–2760

[a] The spectral grasp is given to the nearest wavenumber.

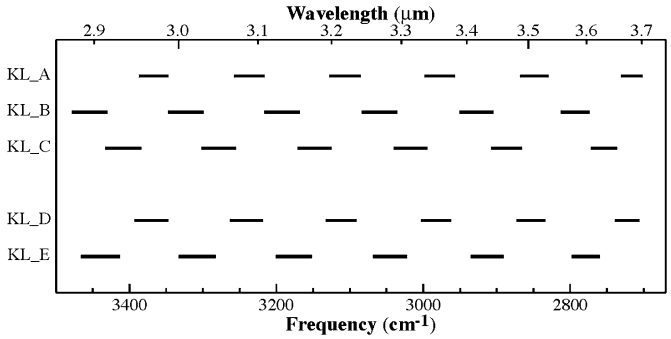

Fig. 2. A graphic representation of the spectral grasp (dark bars) achieved for each grating setting used in this survey (see also Table 2).

transmittance function. The true line flux incident at the top of the terrestrial atmosphere can be determined from the observed flux by correcting for the monochromatic transmittance at the Doppler-shifted line position (obtained from the fully resolved SSP model). Residual spectra of Comet Lee from the five grating settings on two dates comprising this survey, and the normalized atmospheric models (showing atmospheric transmittance as a function of wavelength) are displayed in Fig. 3 (Fig. 3 is shown in its entirety in electronic Supplemental materials).

The residual spectra displayed in Fig. 3 are 9-row (1.74″) extracts centered on the peak comet continuum intensity; at the comet, these spectra represent ∼410 × 1700 km extracts on these dates. This aperture size was chosen to maximize the signal-to-noise ratio of most emission features. Because we are sampling (predominantly) the inner coma, we are most sensitive to the detection of parent species. All distinct emission features (between 3479.0 and 2702.0 cm^{-1}) detected in Comet Lee on two dates are identified by molecule and labeled in Fig. 3 (some are single lines and some are blends of more than one line). These spectra are shifted in wavelength from their actual Doppler-shifted position to the comet rest frame position to facilitate direct comparison with line positions from molecular line atlases and/or laboratory spectra.

Detailed line positions, relative line intensities, signal-to-noise ratios (SNRs), widths, and assignments (where possible) are given in Tables 3 and 4 for UT 1999 Aug. 19.6 and 21.6, respectively (these tables are shown in their entirety in electronic Supplemental materials). SNRs in Tables 3 and 4 are a measure of the emission strengths including effects of atmospheric extinction (dependent on the geocentric Doppler-shift and column burden of absorbing atmospheric species) and wavelength dependent noise variations. The relative line intensities in Tables 3 and 4 (given in arbitrary units) are proportional to line fluxes incident at the top of the terrestrial atmosphere and are a measure of intrinsic line strengths. We emphasize that the conversion of line fluxes within nucleus-centered extracts to absolute production rates and relative abundances is not straightforward—a Q-curve analysis is required (cf. Dello Russo et al., 1998, 2005). Moreover, strong terrestrial absorption features may obscure many additional lines.

Two criteria are used to identify "real" emission features in our spectra. First, a real emission must have a SNR $\geqslant 5.0$ when summed over at least 5-pixels in the spectral dimension (i.e., over 5 columns or ∼0.18–0.26 cm^{-1}). The estimated background-limited noise ($\pm 1\sigma$; this is also referred to as photon noise, or stochastic noise) is shown channel-by-channel in Fig. 3. The noise shown in Fig. 3 does not include errors introduced by misfits between the comet spectra and the (scaled) atmospheric model. These errors are difficult to quantify, but they are generally small compared to the background noise except in the cores (and to a lesser extent the wings) of strong atmospheric lines (these are generally regions of low atmospheric transmittance). For this reason, our second "reality" criterion is that the atmospheric transmittance be $\geqslant$25% (at line center). Based on these criteria we have 545 real emission features in our survey of Comet Lee, many of which were detected on both dates (Tables 3 and 4; note that emissions detected on both dates are counted twice in the total). Molecular progenitors have been identified for 444 of these emissions.

3. Molecular identifications

Molecules within the survey were generally identified and assigned (vibrationally and rotationally) by comparison to published laboratory molecular line lists. In the case of methanol (CH_3OH), where the spectrum is complex and many relevant lines are unassigned, we compared the Lee data directly to laboratory spectra to obtain molecular identifications and line positions. Emissions due to known unresolved components (possibly from the same species) are considered "blended" (the C_2H_6 ν_7 Q-branches are an exception to this; they are a pileup of lines but for simplicity are considered single component in this survey). Blended emissions with known contributions from more than one species are considered multi-species emissions, while any emission (blended or not) that is due to a single molecule is considered a single-species emission (Tables 5, 6). A breakdown of the number and strength of emissions seen in the

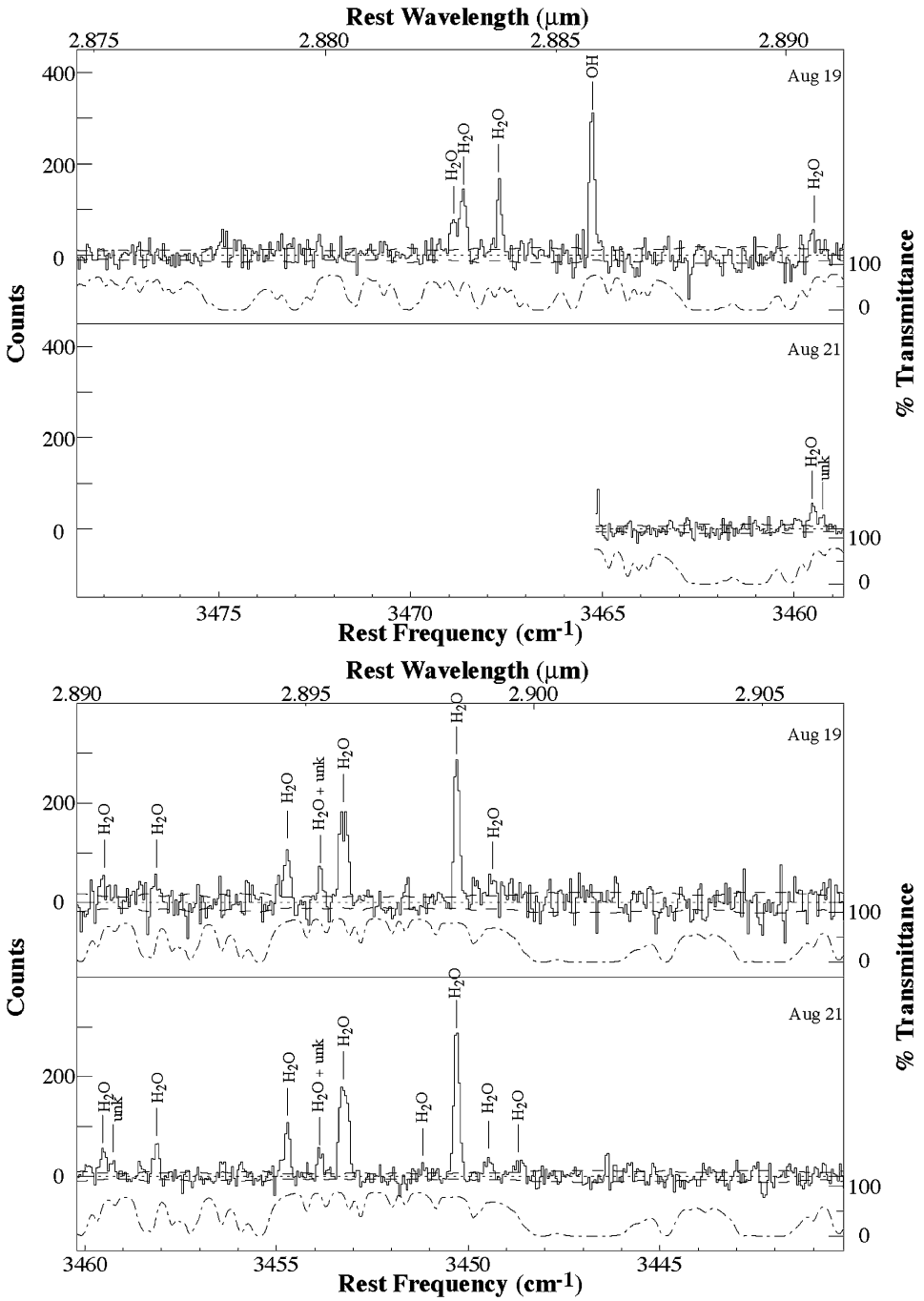

Fig. 3. Example spectra from a high-resolution infrared spectral survey of Comet C/1999 H1 Lee between 2.874 and 3.701 μm on two dates. Continuum-subtracted spectral residuals (solid traces) remain convolved with the atmospheric transmittance. Emission features are noted and molecular assignments are given (unk = unidentified feature). The dashed curves superimposed on the comet residuals are the estimated $\pm 1\sigma$ channel-by-channel "photon" noise; the curves of alternating dashes and dots represent the percent transmittance through the terrestrial atmosphere (right abscissa) as a function of wavelength. The signal intensity for the spectral residuals is given on the left abscissa in counts (arbitrary units). Comet spectra are shifted in wavelength from their actual position (Doppler-shifted) to the comet rest frame position (in cm^{-1} and μm) to facilitate direct comparison to line positions from molecular line atlases and laboratory spectra. The amount that the spectra were shifted (in cm^{-1}) is $(\nu/c)(\Delta_{dot})$, where ν is the frequency (cm^{-1}), c is the speed of light (km/s), and Δ_{dot} is the geocentric Doppler-shift (km/s). The wavelength scale for the synthetic transmittance spectrum is shifted by the same amount. This figure appears in its entirety in Icarus electronic Supplemental material.

Comet Lee survey spectra by molecule is given in Tables 5 and 6.

Several regions have a high density of spectral lines leading to a significant number of multi-species emissions (160 out of 545) within the survey. In general, obtaining quantitative information from multi-species emissions is difficult. However, many multi-species emissions consist of a single dominant component (e.g., some C_2H_6 Q-branches and HCN ν_3 lines); possible minor components are noted for completeness. Multi-species emissions with a dominant component can

Table 3
Examples of detected emissions in Comet C/1999 H1 (Lee) on UT Aug. 19.6, 1999

Rest position[a]		Line int.[b]	SNR[c]	Line width[d]	Molecular assignment[e]			
(cm^{-1})	(μm)				Molecule	Vib.[f]	Rot.[g]	(cm^{-1})[h]
3468.88	2.88277	9.0 (m)	11.7	5	H_2O	101–100	5_{15}–6_{16}	3468.87
						111–110	3_{12}–4_{13}	3468.75
3468.62	2.88299	12.4 (s)	19.7	5	H_2O	200–001	1_{01}–0_{00}	3468.65
						101–100	5_{05}–6_{06}	3468.63
						101–001	2_{02}–2_{11}	3468.53
3467.70	2.88376	17.0 (s)	14.4	8	H_2O	101–100	4_{13}–5_{14}	3467.68
3465.25	2.88579	21.5 (vs)	35.4	7	OH	$1 \rightarrow 0$	P2.5 2^+	3465.26
							P2.5 2^-	3465.26
3459.48[i]	2.89061	4.7 (w)	6.7	6	H_2O	101–001	1_{11}–2_{02}	3459.53
						101–100	4_{31}–5_{32}	3459.49
3458.11[i]	2.89175	5.7 (w)	5.0	6	H_2O	101–001	0_{00}–1_{11}	3458.12
3454.72[i]	2.89459	5.0 (s)	13.6	6	H_2O	101–001	2_{11}–2_{20}	3454.69
3453.85[i]	2.89532	2.7 (w)	7.9	5	H_2O	110–010	3_{13}–4_{22}	3453.88
					Unknown			
3453.25[i]	2.89582	11.5 (vs)	26.9	9 (br)	H_2O	200–100	1_{10}–2_{21}	3453.30
						101–100	2_{02}–3_{21}	3453.15
3450.29[i]	2.89831	13.3 (vs)	33.9	6	H_2O	200–001	1_{10}–1_{11}	3450.29
3449.36[i]	2.89909	3.4 (w)	6.7	6	H_2O	101–100	5_{24}–6_{25}	3449.38

Note. This table appears in its entirety in Icarus electronic Supplemental materials.

[a] The observed rest frequency and wavelength for emissions in the Comet Lee residual extracts.

[b] The observed line intensity incident at the top of the terrestrial atmosphere in arbitrary units (line intensities in flux units can be obtained by contacting NDR) and strength of the emission in the residuals still convolved with the atmospheric transmittance function (in parentheses) over the specified line width: w = 5–8σ; m = 8–12σ; s = 12–20σ; vs > 20σ. Stochastic errors in the line intensity = intensity/SNR, however, there is additional uncertainty (estimated to be at least 10%) in the absolute flux calibration for each order within a setting. In some cases we have (somewhat arbitrarily) treated emissions that are not fully resolved as separate emission lines, the positions of all separately assigned lines are given in this table and indicated by vertical tick marks in Fig. 3.

[c] The signal-to-noise ratio of the detected emissions over the specified line width in the residual spectrum.

[d] The observed width (in pixels) of emission lines in the residual extracts where line intensities were determined. An emission line was considered real when SNR $\geqslant$ 5.0 for line widths $\geqslant$5 pixels and transmittance through the atmosphere at line center was $\geqslant$25%; (br) = line width $\geqslant$9 pixels. The spectral dispersion ($\Delta\nu_{pix}$) in this wavelength range was between −0.036 and −0.052 cm^{-1}/pixel.

[e] Molecular assignments and line positions were obtained from the following references: H_2O positions and assignments (Tennyson et al., 2001; Dello Russo et al., 2004); OH (Maillard et al., 1976; Abrams et al., 1990); NH_3 (Kleiner et al., 1999); HCN (Rothman et al., 1992); NH_2 (Amano et al., 1982a); C_2H_2 (Vander Auwera et al., 1993); CH_2 (Jensen, 1988); CH_3 (Amano et al., 1982b); CH_4 (Féjard et al., 2000; Rothman et al., 1992; Ghérissi et al., 1981; Dang-Nhu et al., 1979); C_2H_6 (Mélen et al., 1993; Pine and Lafferty, 1982); CH_3OH (Xu et al., 1997; Xu, Wang, and Perry, personal communication; Hunt et al., 1991); CH (Bernath, 1987); H_2CO (Reuter et al., 1989). Possible spurious unknowns are labeled (unknown?) (see Section 3.12).

[f] Vibrational assignment (from above references).

[g] Rotational assignment (from above references).

[h] Rest frequencies of assigned molecular emissions (from above references).

[i] Denotes emissions also detected on UT August 21.6.

generally be treated as single-species emissions in quantitative analysis without introducing significant error. Molecular production rates from some detected species in this survey have been previously reported and are summarized in Table 7. Molecules detected in the survey and prospects for detecting and quantifying additional molecules at infrared wavelengths with high-resolution spectroscopy are now discussed.

3.1. H_2O

H_2O can be detected in comets from airborne or space observatories at infrared and submillimeter wavelengths when observing opportunities from these platforms are available (cf. Mumma et al., 1986; Crovisier et al., 1997; Chiu et al., 2001; Lecacheux et al., 2003; Bensch et al., 2004). However, high-resolution infrared spectroscopy is presently the best method for routinely detecting H_2O in comets from generally more accessible ground-based observatories. To avoid extinction from terrestrial water lines, we target lines from non-resonance fluorescence vibrational bands (hot-bands). For more than ten years, this method has been used to target H_2O hot-bands in the K-band near 2 μm (Mumma et al., 1995, 1996; Dello Russo et al., 2002a), and in the M-band near 5 μm (Mumma et al., 1996, 2000, 2001b; Weaver et al., 1999a, 1999b; Dello Russo et al., 2000, 2002a, 2004; Brooke et al., 2003). Although the 2 and 5 μm spectral regions have been important for studying H_2O production in comets, there are several strong water hot-bands in the L-band near 2.9 μm. Water production rates, rotational temperatures and *ortho*-to-*para* ratios (OPRs) based on hot-band lines near 2.9 μm were determined in five comets including C/1999 H1 Lee (Dello Russo et al., 2005; Bonev, 2005; Table 7).

There are several advantages to studying H_2O hot-bands near 2.9 μm. (1) Most molecular species detectable with infrared spectroscopy have their strongest transitions in the L-band, and the large spectral grasp of NIRSPEC over multiple orders allows their sampling simultaneously with H_2O.

Table 4
Examples of detected emissions in Comet C/1999 H1 (Lee) on UT Aug. 21.6, 1999

Rest position[a]		Line int.[b]	SNR[c]	Line width[d]	Molecular assignment[e]			
(cm^{-1})	(μm)				Molecule	Vib.[f]	Rot.[g]	(cm^{-1})[h]
3459.53[i]	2.89057	3.1 (s)	13.3	6	H_2O	101–001	1_{11}–2_{02}	3459.53
						101–100	4_{31}–5_{32}	3459.49
3459.28	2.89078	1.4 (w)	7.5	5	Unknown			
3458.12[i]	2.89174	4.6 (s)	12.5	5	H_2O	101–001	0_{00}–1_{11}	3458.12
3454.72[i]	2.89459	4.7 (vs)	26.2	7	H_2O	101–001	2_{11}–2_{20}	3454.69
3453.87[i]	2.89530	2.0 (s)	13.3	5	H_2O	110–010	3_{13}–4_{22}	3453.88
					Unknown			
3453.25[i]	2.89582	11.8 (vs)	61.7	8	H_2O	200–100	1_{10}–2_{21}	3453.30
						101–100	2_{02}–3_{21}	3453.15
3451.18	2.89756	0.8 (w)	5.8	5	H_2O	101–001	4_{13}–4_{22}	3451.09
3450.30[i]	2.89830	13.0 (vs)	67.5	7	H_2O	200–001	1_{10}–1_{11}	3450.29
3449.46[i]	2.89900	2.2 (m)	9.5	6	H_2O	101–100	5_{24}–6_{25}	3449.38
3448.69	2.89965	3.3 (w)	7.2	8	H_2O	101–100	6_{06}–7_{07}	3448.74
						111–110	5_{15}–6_{16}	3448.72

Note. This table appears in its entirety in Icarus electronic Supplemental materials.

[a] The observed rest frequency and wavelength for emissions in the Comet Lee residual extracts.

[b] The observed line intensity incident at the top of the terrestrial atmosphere in arbitrary units (line intensities in flux units can be obtained by contacting NDR) and strength of the emission in the residuals still convolved with the atmospheric transmittance function (in parentheses) over the specified line width: w = 5–8σ; m = 8–12σ; s = 12–20σ; vs > 20σ. Stochastic errors in the line intensity = intensity/SNR, however, there is additional uncertainty (estimated to be at least 10%) in the absolute flux calibration for each order within a setting. In some cases we have (somewhat arbitrarily) treated emissions that are not fully resolved as separate emission lines, the positions of all separately assigned lines are given in this table and indicated by vertical tick marks in Fig. 3.

[c] The signal-to-noise ratio of the detected emissions over the specified line width in the residual spectrum.

[d] The observed width (in pixels) of emission lines in the residual extracts where line intensities were determined. An emission line was considered real when SNR ⩾ 5.0 for line widths ⩾5 pixels and transmittance through the atmosphere at line center was ⩾25%; (br) = line width ⩾9 pixels. The spectral dispersion ($\Delta\nu_{pix}$) in this wavelength range was between −0.036 and −0.052 cm^{-1}/pixel.

[e] See footnote e in Table 3.

[f] Vibrational assignment (from above references, see Table 3).

[g] Rotational assignment (from above references, see Table 3).

[h] Rest frequencies of assigned molecular emissions (from above references, see Table 3).

[i] Denotes emissions also detected on UT August 19.6.

(2) There are many more hot-bands present near 2.9 μm (in this study we detect lines from six hot-bands) than in the K or M-bands (lines have been detected from two hot-bands in each of these regions). Thus, more H_2O lines are available near 2.9 μm making it easier to determine H_2O production rates, rotational temperatures and OPRs (Dello Russo et al., 2004, 2005). (3) Hot-band lines near 2.9 μm are generally the easiest H_2O lines to detect. They are about a factor of 10–100 stronger than lines near 2 μm, and comparable in strength to lines near 5 μm, however the photon noise at M-band is higher due to the much higher thermal background (telescope plus sky), which can be approximated by a ∼270–290 K Planck function.

One disadvantage of targeting hot-band lines near 2.9 μm is the presence of numerous terrestrial atmospheric water lines (mostly associated with the ν_1 and ν_3 fundamental bands of H_2O) in this spectral region, increasing the chance of extinction due to coincidental overlap with an unassociated telluric feature. Although some H_2O lines in this spectral region are detectable even under conditions of high atmospheric water vapor, the number of detectable lines and the quality of the data are highly sensitive to the atmospheric water burden (Dello Russo et al., 2005). Even under extremely dry atmospheric conditions, much of this spectral region is inaccessible from the ground (see the plot of convolved atmospheric transmittance as a function of wavelength in Fig. 3). When these data were obtained the atmospheric water burden was moderate (∼4 pr-mm; Dello Russo et al., 2005).

H_2O hot-band emission lines are among the most numerous and strongest detected in this survey (Fig. 3, Tables 3–6). Lines from six H_2O hot-bands were present between ∼2.88 and 3.01 μm on both dates (Fig. 3). H_2O line positions were calculated using ro-vibrational energy data (Tennyson et al., 2001). In addition to agreement in line frequency, reasonable agreement in relative line intensities based on developed fluorescence models was necessary for an emission to be identified as pure H_2O (Dello Russo et al., 2004, 2005). Emission features that are significantly stronger than expected were labeled "H_2O + unknown" in Fig. 3, and in Tables 3 and 4. However, as noted in Dello Russo et al. (2004, 2005), uncertainties in the H_2O fluorescence models may account for the discrepancies between the model and data in some cases, without invoking blends with unidentified emissions. Many additional H_2O hot-band lines, obscured by atmospheric extinction in the present survey, have been detected in other comets having geocentric Doppler-shifts different from Comet Lee on these dates (Dello Russo et al., 2004, 2005).

3.2. OH

One traditional method of indirectly determining H_2O production rates is through the detection of its photodissocia-

Table 5
Number and strength of molecular detections in Comet Lee on UT Aug. 19.6

Molecule	Number of single species emissions[a]					Number of multi-species emissions[a]				
	Total	Number of emissions by strength[b]				Total	Number of emissions by strength[b]			
		vs	s	m	w		vs	s	m	w
All	163	9	12	32	110	73	4	3	18	48
Identified	135	9	11	28	87	64	2	3	14	45
Unidentified[c]	28	0	1	4	24	9	2	0	4	3
Securely detected species										
H_2O	26	4	4	5	13	9	2	0	2	5
OH (1–0)	23	3	1	5	14	14	1	1	4	8
OH (2–1)	4	0	0	1	3	4	0	0	0	4
HCN	6	0	0	1	5	1	0	0	1	0
NH_2	7	0	1	3	3	5	0	1	1	3
CH_4	3	0	2	0	1	2	0	0	0	2
C_2H_6	20	2	1	5	12	37	2	2	11	22
CH_3OH	41	0	2	8	31	50	2	2	13	33
H_2CO	4	0	0	0	4	8	0	0	1	7
Species noted but not securely detected[d]										
NH_3	0	0	0	0	0	3	0	0	1	2
C_2H_2	0	0	0	0	0	3	0	0	1	2
CH_2	0	0	0	0	0	3	0	0	0	3
CH_3	1	0	0	0	1	0	0	0	0	0
CH	0	0	0	0	0	4	0	0	0	4

[a] Single species emissions refer to emissions due to a single molecule (emissions due to multiple lines from a single molecule are also considered single species). Single emission features with likely contributions from multiple molecules (even if there is one dominant component) are considered multi species emissions.

[b] vs = very strong, s = strong, m = medium, w = weak. See footnote b in Tables 3 and 4.

[c] There were 37 unidentified emissions on this date: 14 were also detected on UT Aug. 21.6, 23 were detected only on UT Aug. 19.6 (10 out of those 23 were only spectrally covered on UT Aug. 19.6).

[d] There is insufficient evidence to claim detections of these species. These species are included for completeness since they are known comet constituents and they may contribute to some features.

Table 6
Number and strength of molecular detections in Comet Lee on UT Aug. 21.6

Molecule	Number of single species emissions[a]					Number of multi-species emissions[a]				
	Total	Number of emissions by strength[b]				Total	Number of emissions by strength[b]			
		vs	s	m	w		vs	s	m	w
All	222	16	26	66	114	87	9	22	33	23
Identified	170	15	24	54	77	75	8	18	31	18
Unidentified[c]	52	1	2	12	37	12	1	4	2	5
Securely detected species										
H_2O	20	6	4	6	4	10	1	5	2	2
OH (1–0)	20	0	8	5	7	11	2	3	5	1
OH (2–1)	11	0	0	4	7	4	0	1	1	2
HCN	11	0	1	9	1	2	1	0	1	0
C_2H_2	4	0	0	0	4	3	1	0	1	1
NH_2	10	0	1	3	6	7	1	1	2	3
CH_4	4	2	1	0	1	2	0	1	1	0
C_2H_6	15	3	3	3	6	46	5	9	22	10
CH_3OH	67	4	6	23	34	63	6	15	24	18
H_2CO	6	0	0	1	5	11	0	4	3	4
Species noted but not securely detected[d]										
NH_3	0	0	0	0	0	1	0	0	0	1
CH_2	1	0	0	0	1	5	0	2	3	0
CH_3	1	0	0	0	1	0	0	0	0	0
CH	0	0	0	0	0	5	1	0	2	2

[a] Single species emissions refer to emissions due to a single molecule (emissions due to multiple lines from a single molecule are also considered single species). Single emission features with likely contributions from multiple molecules (even if there is one dominant component) are considered multi species emissions.

[b] vs = very strong, s = strong, m = medium, w = weak. See footnote b in Tables 3 and 4.

[c] There were 64 unidentified emissions on this date: 14 were also detected on UT Aug. 19.6.

[d] There is insufficient evidence to claim detections of these species. These species are included for completeness since they are known comet constituents and they may contribute to some features.

Table 7
Molecular production rates in Comet Lee

Species	Q (10^{27} s^{-1})[a]	T_{rot} (K)[b]	OPR[c]	Relative abundance
H_2O[d]	143.1 ± 13.3	76^{+4}_{-3}	2.5 ± 0.5	100
CH_3OH[e]	2.3 ± 0.2	(75)		1.6 ± 0.2
CH_4[f]	1.62 ± 0.32	(75)		1.13 ± 0.25
C_2H_6[e]	1.02 ± 0.05	80^{+25}_{-19}		0.71 ± 0.07
HCN[e]	0.29 ± 0.02	72 ± 8		0.20 ± 0.02
C_2H_2[e]	0.34 ± 0.03	(75)		0.24 ± 0.03

[a] Production rates are for UT Aug. 21.6. Production rates for H_2O and CH_4 were also determined on UT Aug. 19.6: Q (H_2O) = 133.5 ± 12.8, Q (CH_4) = 1.84 ± 0.42, $CH_4/H_2O = (1.38 \pm 0.34)\%$ (Gibb et al., 2003; Dello Russo et al., 2005). Production rates for other species on both dates will be reported in future publications.

[b] Rotational temperatures in parentheses are assumed. T_{rot} for H_2O on UT Aug. 19.6 was 80^{+6}_{-4} K (Dello Russo et al., 2005).

[c] The OPR for H_2O on UT Aug 19.6 was 2.5 ± 0.5 (Dello Russo et al., 2005). A statistical equilibrium nuclear spin temperature was assumed for other molecules with multiple nuclear spin species.

[d] Values from Dello Russo et al. (2005).

[e] Values from Mumma et al. (2001a). Mixing ratios are updated based on Q (H_2O) from Dello Russo et al. (2005).

[f] Values from Gibb et al. (2003). CH_4 mixing ratios are updated based on Q (H_2O) from Dello Russo et al. (2005).

tion product OH at near-ultraviolet and radio frequencies (cf. Schleicher and A'Hearn, 1982; Crovisier et al., 2002). OH transitions can also be detected at infrared wavelengths either via fluorescent emission or prompt emission (Weaver and Mumma, 1984; Crovisier, 1989; Bockelée-Morvan and Crovisier, 1989). In the prompt emission mechanism, photodissociation of H_2O produces OH radicals in vibrationally-excited and rotationally-hot states (Carrington, 1964; Yamashita, 1975; Andresen et al., 1984; Hausler et al., 1987; Engel et al., 1988; Nizkorodov et al., 2003). The distribution of OH in the coma produced via prompt emission should trace that of the parent H_2O, while OH produced via fluorescence should have a more extended distribution (cf. Crovisier, 1989). With high-resolution spectroscopy, OH emission has been detected from the ground at infrared wavelengths (Brooke et al., 1996; Magee-Sauer et al., 1999; Mumma et al., 2001a; Gibb et al., 2003). A complete quantitative analysis of prompt emission from the OH multiplet near 3046 cm^{-1} (including a direct comparison between the OH and the H_2O spatial distributions), and its use as a tracer for H_2O production, was done for Comet Lee on both dates covered by this survey (Bonev et al., 2004). A comprehensive analysis of OH lines in two other comets from additional detected multiplets is presented in Bonev (2005).

Multiple emission lines from two bands of OH (1–0 and 2–1), spanning the entire spectral grasp of our survey were detected in Comet Lee on both dates. Line positions and assignments for OH lines were obtained from Maillard et al. (1976) and Abrams et al. (1990). The OH emissions detected in this survey can be split into two groups; those that are entirely due to prompt emission, and those that may be a mixture of prompt and fluorescent emission. For the P-branch region of the (1–0) band, all OH lines at wavelengths longer than ~2.95 μm should be entirely due to prompt emission, while those in our survey between 2.88 and 2.95 μm may be mixed (Bockelée-Morvan and Crovisier, 1989). These two mechanisms may be differentiated by comparing the spatial distribution of OH and H_2O lines in the coma: Prompt OH should trace the parent (H_2O) while fluorescent OH will display a flatter (more extended) spatial distribution (Bonev et al., 2004; Bonev, 2005). A study on the spatial distribution of OH is beyond the scope of this paper (see Bonev et al., 2004; Bonev, 2005, for additional details).

Models of prompt emission by OH created in rotationally excited states suggested that emission from OH (1–0) at wavelengths longer than ~3.1 μm should be negligible if OH is produced with a rotational temperature of 300 K (Bockelée-Morvan and Crovisier, 1989). We note however that earlier laboratory measurements predict a much hotter distribution in the $v' = 1$ vibrational level based on dissociation of H_2O at 300 K via absorption of Lyman-α (Carrington, 1964; Yamashita, 1975) or in the first absorption band of water (Andresen et al., 1984; Hausler et al., 1987). Detection of OH (1–0) lines out to 3.66 μm in this survey confirms a distribution much hotter than 300 K upon creation. Lines from the (2–1) band of OH were generally several times weaker than the corresponding (1–0) lines, and detection of high-J lines from the (2–1) band also suggests a prompt emission mechanism.

3.3. HCN

Comet impacts were likely an important source of organic molecules on the early Earth (cf. Delsemme, 2000). The presence of HCN in comets is significant since it is an important intermediary for synthesis of biochemical compounds (cf. Oro et al., 1992). HCN has been detected and quantified in comets at millimeter wavelengths for twenty years (Despois et al., 1986; Schloerb et al., 1986; Biver et al., 2002). Since HCN has a strong vibrational band near 3 μm, the prospect of detecting HCN in comets at infrared wavelengths was considered even before spectrometers of sufficient sensitivity and spectral resolving power were available (Crovisier, 1987). Since its initial detection at infrared wavelengths in comet Hyakutake, HCN has been routinely measured in comets at infrared wavelengths (Brooke et al., 1996, 2003; Magee-Sauer et al., 1999, 2002a, 2002b; Weaver et al., 1999a; Mumma et al., 2001a, 2001b, 2003). We note that production rates for HCN measured at millimeter and infrared wavelengths often do not agree, with infrared values generally about a factor of two higher (Magee-Sauer et al., 2002a; Biver et al., 2002). These differences are perhaps not surprising when comparing absolute production rates from different wavelength regimes where observing platform and approach, beam sizes, and modeling complexity differ (Magee-Sauer et al., 2002a). However, millimeter production rates can increase if electron collisions are included possibly removing much of the discrepancy (Lovell et al., 2004).

In addition to its biogenic importance, HCN is likely a major source of CN seen in many comets (cf. A'Hearn et al., 1995; Fink and Hicks, 1996). However, the relationship of HCN to CN in comets is not completely understood. Rauer et al. (1997) claimed that the HCN in Hale–Bopp detected during observations at large heliocentric distances could account for all of the

measured CN. Closer to perihelion, however, the HCN/CN ratio seemed to indicate too much HCN in Hale–Bopp to account for the observed amount of CN (Ziurys et al., 1999). Studies comparing isotopic ratios of HCN in Hale–Bopp with CN (in Hale–Bopp and three other comets) suggest other parents are likely important for the formation of CN in cometary comae (Manfroid et al., 2005). An in-depth study on the relationship of HCN to CN in eight comets revealed that HCN could explain the observed CN in some comets but not others (Fray et al., 2005).

In many comets there is evidence that much of the measured CN is produced from grains in the coma, rather than from nuclear ices (A'Hearn et al., 1995). It may be that a fraction of HCN itself might be produced in the coma by grains, but at this time there is no clear evidence for a significant distributed component of HCN in comets. Infrared studies of the spatial distribution of HCN along the slit have shown no evidence for a distributed source (cf. Magee-Sauer et al., 1999, 2002a). Interferometric studies of HCN at millimeter wavelengths show possible evidence for a small contribution (up to ∼20%) from a distributed source (Wright et al., 1998; Veal et al., 2000), however contributions from coma chemistry or temporal variability may account for small deviations from a Haser profile. The importance of HCN in explaining the observed CN in comets must be examined on a case-by-case basis using direct comparison of CN and HCN production rates and spatial distributions (see Fray et al., 2005).

Obtaining accurate molecular production rates requires knowledge of the rotational distribution, and typically a sufficient number of HCN lines can be detected near 3.0-μm to obtain a rotational temperature (Magee-Sauer et al., 1999, 2002a; Mumma et al., 2001a). In this survey, multiple lines of the ν_3 band of HCN have been detected, and quantitative results for HCN on UT Aug. 21 have been reported elsewhere (Mumma et al., 2001a; Table 7). A preliminary comparison based on the presence and relative intensities of HCN lines on both dates (Fig. 3, Tables 3, 4) suggests that the HCN production rate may have been somewhat lower on UT Aug. 19.6 compared to Aug. 21.6. We note that H_2O production rates on these dates agree within error (Dello Russo et al., 2005), so the HCN/H_2O ratio may have changed between these dates. A detailed quantitative study of HCN on UT Aug. 19.6 (including Q-curve analysis) will be needed to test this possibility, and is deferred to a future publication.

We note that, as was the case with H_2O hot-band lines, the number of detectable HCN lines and the data quality depend on the atmospheric water burden. Also, the 3 μm spectral region in comets has a high density of emission features, resulting in spectral confusion (Fig. 3). Many emissions from known molecules (e.g., HCN, C_2H_2, NH_3, NH_2, OH), as well as unknown emissions are present in this region. Blends with known constituents are noted in Tables 3 and 4. In most cases, HCN is the dominant constituent in any blend and many HCN lines are generally detected, so blends are unlikely to significantly affect the infrared analysis of HCN in comets. Positions and assignments for HCN lines detected in this survey were obtained from the HITRAN 1992 database (Rothman et al., 1992).

3.4. C_2H_2

Acetylene (C_2H_2) is a symmetric hydrocarbon, so it can be observed only at infrared wavelengths. Reactions of CN and C_2H radicals with unsaturated hydrocarbons like C_2H_2 can form complex organics such as amino acids (cf. Kaiser and Balucani, 2002), so acetylene has potential importance to astrobiology. Also, C_2H_2 is likely a major source of the C_2 detected in a large number of comets observed since the 1970s with narrowband photometry (cf. A'Hearn et al., 1995; Fink and Hicks, 1996). Presently, the parentage of C_2 is not completely understood (cf. Combi and Fink, 1997).

High-resolution spectra of Comet Hyakutake obtained with the Hubble Space Telescope found that the C_2 had hot vibrational and rotational excitation, similar to that observed when C_2H_2 is photodissociated in the laboratory (Sorkhabi et al., 1997). However, it is possible that the hot vibrational and rotational excitation of C_2 is due to fluorescent pumping at optical wavelengths rather than being the initial distribution following photolysis of C_2H_2. It is also possible that photodissociation of other C_2-bearing molecules (e.g., C_2H_4, C_2H_6) could produce electronically-excited C_2 fragments whose emission might contribute to the observed Hyakutake spectra (Crovisier, 1998). A study in Comet Hale–Bopp for heliocentric distances $\geqslant$2.9 AU concluded that the formation of C_2 was dominated by photodissociation and electron impact dissociation of C_2H_2 (Helbert et al., 2005). In many comets the spatial distribution of C_2 is flatter than expected from simple photodissociation of a parent molecule (cf. Combi and Delsemme, 1986), implying that release from dust grains having organic mantles may contribute to the observed C_2 (cf. Wyckoff et al., 1988; Combi and Fink, 1997). Direct comparison of C_2 abundances with potential parents such as C_2H_2 is important for resolving the parentage of cometary C_2.

Acetylene has been detected in comets with high-resolution infrared spectroscopy near 3.0 μm (Brooke et al., 1996, 2003; Magee-Sauer et al., 1999, 2002a, 2002b; Weaver et al., 1999a; Mumma et al., 2000, 2001b). Due to Fermi-type interaction coupling between ν_3 and $\nu_2 + \nu_4 + \nu_5$ vibrational bands (Lafferty and Thibault, 1964; Vander Auwera et al., 1993), lines from these bands may rival each other in intensity, and detections of lines from both bands have been reported in comet spectra (cf. Brooke et al., 2003). C_2H_2 has *ortho* and *para* spin species (for statistical equilibrium, odd-J lines are 3 times stronger than even-J lines for these two bands), so a determination of OPR is possible if enough lines of both spin species can be detected.

Detecting multiple strong C_2H_2 lines in comets has been and likely will continue to be problematic. There are several reasons for this difficulty: (1) The low abundance of C_2H_2 in comets (typically $\leqslant$0.2% with respect to H_2O), coupled with only moderate strengths for the two bands make these lines relatively weak in comet spectra (e.g., Fig. 3); the weaker even-J (para) lines are particularly difficult to detect. (2) Spectral confusion (or complexity) in the 3.0 μm region causes some of the C_2H_2 lines to be significantly blended with other species (e.g., HCN, NH_2, OH; see Fig. 3, Tables 3, 4). (3) Atmospheric transmit-

tance is generally poor in the 3.0 μm region causing obscuration of many C_2H_2 lines (Fig. 3). In this survey, four unblended lines of C_2H_2 were detected on UT August 21.6 (Tables 4 and 6). The C_2H_2 production rate in Comet Lee on this date has been previously reported (Mumma et al., 2001a; Table 7), but an insufficient number of lines were detected for the determination of a meaningfully constrained rotational temperature, much less an OPR. No firm detections of unblended C_2H_2 emissions are seen in spectra from UT August 19.6, although three C_2H_2 lines may contribute to blended multi-species emission features (Table 5). Positions and assignments for C_2H_2 lines detected in this survey were obtained from Vander Auwera et al. (1993) (Tables 3, 4).

3.5. NH_3

Ammonia is another important biogenic molecule since it was likely an intermediary for synthesis of amino acids on the early Earth. A tentative detection of NH_3 was claimed in Comet C/1983 H1 IRAS–Araki–Alcock through its 24 GHz inversion line (Altenhoff et al., 1983). Its detection was subsequently claimed in Halley from Giotto mass spectrometer measurements (Allen et al., 1987; Meier et al., 1994), and through radio inversion lines in Comets Hyakutake and Hale–Bopp (Palmer et al., 1996; Bird et al., 1997, 1999; Hirota et al., 1999). Ammonia has been detected at infrared wavelengths near 3.0 μm in Comets Hale–Bopp, 153P/Ikeya–Zhang (C/2002 C1), and C/2002 T7 (Magee-Sauer et al., 1999; Magee-Sauer et al., in preparation). Apparently well-constrained NH_3 spin temperatures have been indirectly determined in comets through measurements of the NH_2 radical with the assumptions that OPR is conserved upon photodissociation and that NH_2 is the sole parent of NH_3 (Kawakita et al., 2001, 2002, 2004). However, it is not clear if other sources of uncertainty in addition to photon noise were considered when errors for these spin temperatures were derived (see Section 4.2 for discussion of other possible sources of error). NH_3 has two nuclear spin species (A $(I = 3/2)$ and E $(I = 1/2)$), so in principal, spin temperatures can be directly determined for NH_3 in comets if a sufficient number of lines from each spin species is detected.

NH_3 was not definitively detected in this survey on either date, although it may contribute to some blended multi-species emissions (Tables 5, 6). Reasons for the difficulty in detecting NH_3 in high-resolution infrared spectra near 3.0 μm are the same as for C_2H_2 (see discussion in Section 3.4). Line positions for NH_3 used in this survey were obtained from Kleiner et al. (1999).

3.6. NH_2

Ammonia production rates in comets can be indirectly investigated from photodissociation products, and bands of NH_2 (observed at visible wavelengths) have been used for this purpose (cf. Wyckoff et al., 1991; Feldman et al., 2005). The detection of NH_2 in Comet Lee on UT August 21.6 was originally noted in Mumma et al., 2001a. Here we report the detection of multiple lines from two bands (ν_1 and ν_3) of NH_2 on both dates of our survey between ~3.01 and 3.19 μm (Fig. 3, Tables 3–6). We again note that poor atmospheric transmittance and spectral confusion near 3.0 μm will limit the number of detectable and unblended lines. The density of lines from other species is lower between 3.05 and 3.19 μm so spectral confusion is less of an issue, however, atmospheric transmittance remains poor throughout much of this region (Fig. 3). Positions and assignments for NH_2 lines detected in this survey were obtained from Amano et al. (1982a) (Tables 3, 4). As in the case of OH, spatial studies of NH_2 can test whether its presence in the coma is due to a prompt or fluorescence emission mechanism; however, we note that its probable parent, NH_3, was not definitively detected in our survey. We also note that a preliminary comparison based on the presence and relative intensities of NH_2 lines on both dates (Fig. 3, Tables 3, 4) suggests that NH_2 may have been somewhat more abundant on UT Aug. 19.6 compared to Aug. 21.6. A detailed analysis of NH_2 is deferred to a future publication.

3.7. CH_4

Methane is the simplest member of the saturated hydrocarbon homologous series C_nH_{2n+2}, and its abundance in comets relative to others in the series can reveal information about how hydrocarbons were formed in the early solar nebula (Mumma et al., 1996). CH_4 is also highly volatile, so its relative abundance in comets may provide clues about the region of formation and processing history of cometary ices (cf. Gibb et al., 2003). The electronic band systems of CH_4 are predissociated so it is not detectable at UV wavelengths. As a symmetric hydrocarbon, it lacks a permanent dipole moment so it is not detectable at radio wavelengths; however, it has a strong infrared fundamental band (ν_3) near 3.3 μm, which has been the target of observational searches in comets. Attempts to detect the ν_3 band of CH_4 were first made in Comets C/1973 E1 (Kohoutek) and 1P/Halley (Roche et al., 1975; Kawara et al., 1988; Drapatz et al., 1987). A more stringent upper limit in Halley was obtained from analysis of mass spectroscopic data from the Giotto spacecraft (Altwegg et al., 1994). A marginal detection of CH_4 was claimed in C/1986 P1 (Wilson) (Larson et al., 1989) and an upper limit of 0.31% relative to water was reported for Comet Levy (Brooke et al., 1991a). With high-resolution infrared spectroscopy, CH_4 was first unambiguously detected in Comet Hyakutake (Mumma et al., 1996), and subsequently in several other comets with abundances (relative to H_2O) varying by more than an order of magnitude (Weaver et al., 1999a; Mumma et al., 2001a, 2001b; Gibb et al., 2003; Brooke et al., 2003; Kawakita et al., 2003, 2005). CH_4 (both solid and gas phase) has been detected towards star-forming regions (Lacy et al., 1991; Boogert et al., 2004, 1996), and abundances can vary considerably towards massive protostars, so variations in cometary CH_4 abundances may trace physical differences in the early protoplanetary disk (Gibb et al., 2003; Boogert et al., 2004).

Initial quantitative analysis of CH_4 in Comet Lee was done for one date (Mumma et al., 2001a). Recently, a fluorescence model for CH_4 was developed and applied to data obtained on

both dates within this survey and to several other comets (Gibb et al., 2003; Table 7). In principal, CH_4 should be one of the easiest volatile species to detect at infrared wavelengths since it is generally abundant in comets (the observed range is 0.2–1.4% relative to H_2O) and its ν_3 band is strong. However, CH_4 has a strong terrestrial component, which makes it difficult to detect in comets unless the absolute value of the geocentric Doppler-shift (Δ_{dot}) of the comet is adequately large. Typically $|\Delta_{dot}|$ between ∼15 and 40 km s^{-1} is adequate for the detection of a few low-J lines, while larger absolute Doppler-shifts are needed to detect additional lines. Also, lines with $J'' \geqslant 2$ have multiple components that are usually blended even at the high resolving power of spectra such as those presented in this study. For these reasons, CH_4 rotational temperatures and spin temperatures (CH_4 has three spin species) are very difficult to constrain even with relatively large absolute cometary Doppler-shifts. A well-constrained spin temperature was reported for CH_4 in Comet C/2001 Q4 (Kawakita et al., 2005), however it is not clear if uncertainties other than photon noise were included and how the rotational temperature and spin temperature (and their errors) were decoupled. In our survey ($\Delta_{dot} \sim -29$ km s^{-1}), we detected several strong, low-J lines of CH_4 on both dates (Fig. 3, Tables 3–6). While atmospheric transmittance provides a major limitation for the detection of ν_3 CH_4 lines, spectral confusion (due to the higher density of C_2H_6 and CH_3OH lines) becomes an additional hindrance to the detection of P-branch lines (Fig. 3). Positions and assignments for the ν_3 band have been widely published (cf. Dang-Nhu et al., 1979; Ghérissi et al., 1981; Rothman et al., 1992; Féjard et al., 2000).

3.8. CH_3, CH_2, and CH

The radicals CH_3, CH_2, and CH are photodissociation products of CH_4 and other hydrocarbon species. CH bands have been detected in comets at visible wavelengths (cf. Arpigny et al., 1987; Meier et al., 1998a), and CH_2 was detected in Comet Halley from Giotto mass spectrometer data (Altwegg et al., 1994). CH_3 has transitions at vacuum ultraviolet and infrared wavelengths, but has not yet been unambiguously detected in a comet. These radicals have bands with lines in our survey region: CH_3 (ν_3), CH_2 (ν_1, ν_3), and CH (1–0), however, definitive detections were not attained for them (Tables 5, 6). We note that our spectral extracts weight contributions from the inner coma heavily, so they are not as sensitive to daughter species. Line positions and assignments in Tables 3 and 4 were obtained from: CH_3 (Amano et al., 1982b), CH_2 (Jensen, 1988), and CH (Bernath, 1987).

3.9. C_2H_6

C_2H_6 is next in the homologous series of saturated hydrocarbons after CH_4, and like CH_4 is only detectable at infrared wavelengths. With high-resolution infrared spectroscopy, C_2H_6 was first detected in Comet Hyakutake (Mumma et al., 1996), and has been observed routinely in subsequent comets (Weaver et al., 1999a; Mumma et al., 2000, 2001a, 2001b; Dello Russo et al., 2001, 2002a, 2002b; Brooke et al., 2003; Kawakita et al., 2003). The high abundance of C_2H_6 relative to CH_4 and C_2H_2 seen in many comets to date may suggest that C_2H_6 in comets formed via H-atom addition reactions on grains (Mumma et al., 1996). Laboratory studies confirm that C_2H_6 can be formed with high efficiency via H-atom addition reactions to C_2H_2 and C_2H_4 ices (Hiraoka et al., 2000). Alternatively, Notesco et al. (1997) showed that relative abundances of C_2H_6 and CH_4 comparable to those found in Comet Hyakutake can be simulated in the laboratory by trapping these gases in water ice at ∼65 K. However, recent laboratory studies more applicable to the interstellar and solar nebula environments than Notesco et al. (1997) suggest a temperature of ∼25 K for ice grains that accreted into comets (Notesco and Bar-Nun, 2005). Comparison of the relative abundances of C_2H_2, CH_4, and C_2H_6 will continue to be important in constraining comet formation scenarios.

Although less abundant than many volatile constituents, C_2H_6 is generally the most easily detected species after H_2O at infrared wavelengths. The ethane ν_7 Q-branches near 3.35-μm are very strong due to a pile-up of many lines, and unlike CH_4, the terrestrial C_2H_6 component is very weak, so no specific geocentric Doppler-shift is needed for its detection. So, for faint comets with small geocentric Doppler-shifts (e.g., most short-period comets when they are near peak productivity), C_2H_6 is a primary target for sampling hydrocarbon chemistry at infrared wavelengths, and it is a major contributor (along with CH_3OH) to the 3.2–3.6 μm X–CH feature seen in low-resolution studies of comets (see Section 4.3).

Strong C_2H_6 ν_7 Q-branches are prominent in our spectral survey data on both dates (Fig. 3). Many weaker lines of C_2H_6 are also present, e.g., from ν_7 between ∼3.31 and 3.39 μm, $\nu_8 + \nu_{11}$ between ∼3.36 and 3.40 μm, and ν_5 between ∼3.42 and 3.47 μm (Fig. 3, Tables 3, 4). In addition, there are many lines from other species in this region (CH_3OH lines being the most ubiquitous), adding to the severe spectral confusion seen in high-resolution comet data at these wavelengths (Fig. 3). As a result, blended C_2H_6 emissions outnumber pure ones on both dates of our survey (Tables 5, 6). Although many emissions in this region are due to blends, spectral confusion is less important for the Q-branches (the exception being $^RQ_3$ at 2996.87 cm^{-1}), because they are generally significantly stronger than any features with which they are blended. For analysis of other C_2H_6 lines, blends can contribute significantly, so caution must be used in any quantitative analysis of weaker C_2H_6 lines. Positions and assignments for C_2H_6 lines detected in this survey are noted in Tables 3 and 4 (Pine and Lafferty, 1982; Mélen et al., 1993).

3.10. CH_3OH

Methanol was first detected in the interstellar medium in the gas-phase (Ball et al., 1970). Gas-phase methanol has since been detected in hot cores and in icy grain mantles near embedded protostars. Its abundance relative to water ranges from ∼5–30% in high-mass protostars (Brooke et al., 1999; Dartois et al., 1999) and 15–25% in some low-mass protostars (Pontoppidan et al., 2003). Thus, the presence of CH_3OH in comets is to be expected. Low-resolution spectra of Comet

Halley revealed a new emission feature near 3.52 μm. This feature was assigned to an oxygen-containing organic molecule, possibly CH_3OH or H_2CO (Knacke et al., 1986). The presence of CH_3OH in comets was confirmed through detection of the ν_3 band in comets at infrared wavelengths (Hoban et al., 1991, 1993; Davies et al., 1993; DiSanti et al., 1995), and the detection of rotational lines near 145 GHz (Bockelée-Morvan et al., 1991, 1994). Recently, CH_3OH has been detected in many comets at radio wavelengths (cf. Biver et al., 2002) and with high-resolution infrared spectrometers (cf. Mumma et al., 2001a; DiSanti et al., 2002; Brooke et al., 2003). A CH_3OH production rate was obtained in Comet Lee on UT 1999 August 21.6 based on analysis of the ν_3 Q-branch intensities (Mumma et al., 2001a; Table 7).

Methanol lines are ubiquitous between 3.30 and 3.53 μm in our survey data, contributing to at least 220 of the 545 total emission features seen (Tables 5, 6). The CH_3OH lines seen in Lee are due to ν_2, ν_3, and ν_9 fundamental bands and the $2\nu_4$ overtone band. Other lines are also seen that, although unassigned, are likely due to additional overtone and combination bands (e.g., $\nu_5 + \nu_{10}$, $\nu_4 + \nu_5$, $\nu_4 + \nu_{10}$, $2\nu_5$, $2\nu_{10}$) present at these wavelengths. The 3.30–3.53 μm spectral region in comets is characterized by severe spectral confusion due to the high density of lines (primarily CH_3OH and to a lesser extent C_2H_6), which severely limits the ability to isolate and detect other species with bands in this wavelength region. Detecting other less abundant hydrocarbon species in this region is dependant on the development of accurate line-by-line low-temperature fluorescence models for all contributing CH_3OH bands. Modeling efforts are only in their initial stages, owing to the complexity of this problem (Bockelée-Morvan et al., 1994; Brooke et al., 2003).

For some relevant bands of CH_3OH, line positions and assignments are not available or incomplete, so identification and assignment of CH_3OH lines in our spectra was accomplished by two means. (1) Literature values were used when available. Positions and assignments were available for some lines of ν_3 (Xu, Wang and Perry, personal communication; Hunt et al., 1991), ν_2, ν_9, and $2\nu_4$ (Xu, Wang and Perry, personal communication; Xu et al., 1997). (2) We compared our comet spectra with a laboratory FTIR spectrum of CH_3OH at 190 K convolved to the approximate resolution of the comet spectra (Fig. 4). Li-Hong Xu obtained this laboratory spectrum at the National Research Council Facilities in Ottawa with a modified Bomem Fourier transform spectrometer ($\Delta\nu \sim 0.0025$ cm^{-1}). This allowed us to confirm that many unassigned lines within our data corresponded to strong methanol features in the laboratory data. Emission lines in our dataset identified strictly by comparison to the laboratory spectrum were assigned to CH_3OH with a question mark under the columns for vibrational and rotational assignments in Tables 3 and 4. We use this technique for identifying probable CH_3OH features in our comet spectra, but we note that the rotational temperature of CH_3OH in the coma of Comet Lee during these observations was likely ~75 K, so relative intensities of lines in comet and laboratory spectra cannot be directly compared. A laboratory spectrum of C_2H_6 at 119 K (Pine and Lafferty, 1982) was also used for comparison in some spectral regions to help disentangle CH_3OH and C_2H_6 contributions in the survey data (Fig. 4).

3.11. H_2CO

H_2CO was tentatively detected in the IKS low-resolution spectrum of Comet Halley (Moroz et al., 1987; Combes et al., 1988), and application of new fluorescence models later confirmed its detection while also establishing its low rotational temperature (Mumma and Reuter, 1989). It is likely that both monomeric and polymeric forms of formaldehyde are present in comets, but their relative abundances are poorly constrained (Cottin et al., 2004). H_2CO has been detected in many comets at radio wavelengths (cf. Biver et al., 2002), and in some comets there is a significant distributed source in the coma, for example Halley (Eberhardt, 1999) and Hale–Bopp (Biver et al., 1999; Wink et al., 1999). H_2CO has infrared-active bands near 3.5–3.6 μm (ν_1 and ν_5), and line-by-line fluorescence models developed for a few rotational temperatures were used to interpret low-resolution spectra of Comet Halley (Reuter et al., 1989; Mumma and Reuter, 1989). Recently, H_2CO has been definitively detected at infrared wavelengths with high-resolution spectroscopy (DiSanti et al., 2002). In the wavelength regime covered by this survey, lines from both H_2CO ν_1 and ν_5 were detected (Tables 5, 6; line positions and assignments for H_2CO were taken from Reuter et al., 1989). H_2CO has many observable lines between 3.42 and 3.64 μm, however, it is very difficult to unambiguously detect it between 3.46 and 3.55 μm due to the high density of lines from the ν_3 band of CH_3OH. Emissions from the ν_1 band of H_2CO, centered near 3.6 μm are generally easier to detect since they are in a region of greatly reduced spectral confusion (order 21 in this study). Data from Comet C/2002 T7 (LINEAR) obtained with CSHELL at the NASA-IRTF was compared with modeled line intensities for a range of temperatures, thereby validating and extending the model and permitting accurate measures of rotational temperatures and production rates (DiSanti et al., 2006).

As is the case for water, H_2CO has *ortho* and *para* species, so if a sufficient number of lines from each species are detected, an OPR can be determined. We note that the lowest *ortho* level lies significantly closer to the lowest *para* level (the ground rotational state) in the case of H_2CO compared with H_2O, thus a non-equilibrium value (i.e., OPR < 3.0) corresponds to a lower spin temperature ($\leqslant$15 K). A more detailed and quantitative analysis of data near 3.6 μm in Comet Lee will be included in a future publication detailing infrared H_2CO detections in several comets observed with NIRSPEC and/or CSHELL (DiSanti et al., in preparation).

3.12. Unidentified features

After comparing positions of emission features to line lists and laboratory spectra, many (101 out of 545 lines in our survey) remain partially or completely unidentified (labeled "unk" in Fig. 3, see also Tables 3–6). Of the 101 unknown features, 28 were detected on both dates (14 on each date), 50 were detected only on Aug. 21.6, and 23 were detected only on Aug. 19.6

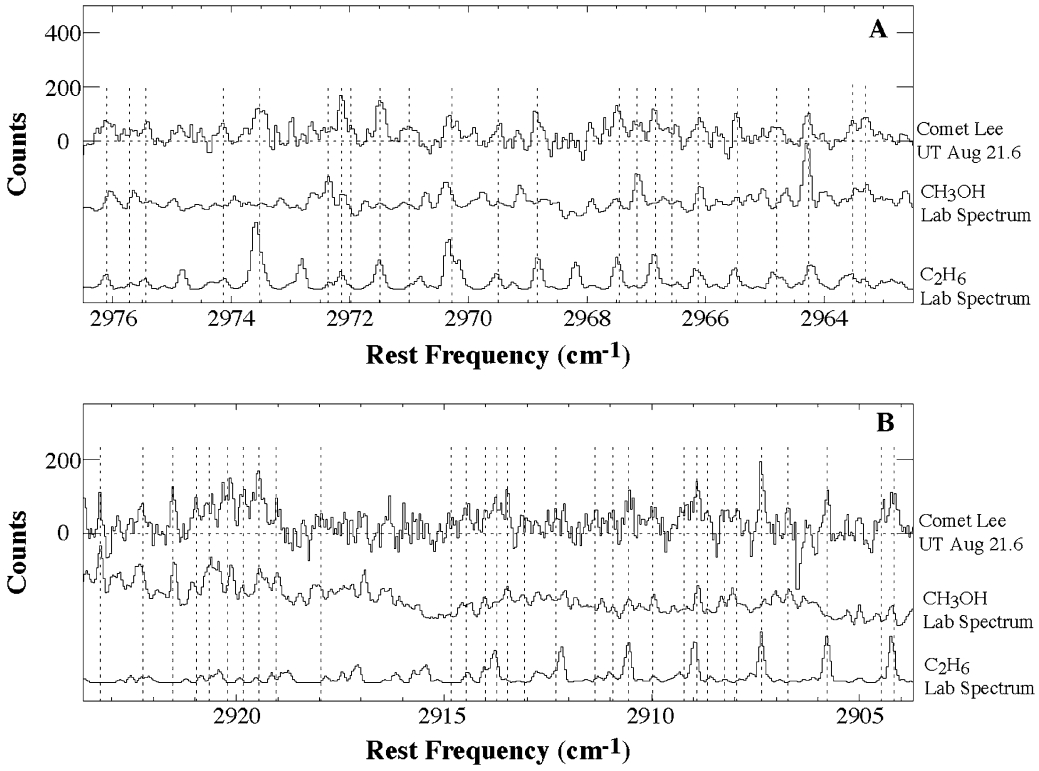

Fig. 4. A comparison of Comet Lee spectra near (A) 3.367 and (B) 3.432 μm on UT 1999 August 21.6 with laboratory spectra of CH_3OH at 190 K (Xu) and C_2H_6 at 119 K (Pine and Lafferty, 1982). Vertical lines indicate the positions of emission features as listed in Table 4. As in Fig. 3, spectra are shifted in wavelength to the comet rest frame. The CH_3OH laboratory spectrum was used for identification purposes only. Detailed fluorescence models will be needed to explain relative intensities of CH_3OH lines.

(and 13 of those had rest frequencies that were covered on both dates). Detecting additional emissions on UT Aug. 21.6 (including unknowns) is not surprising since more time on-source was obtained per grating setting as compared to Aug. 19.6 (Table 1). The 50 unknown emissions unique to Aug. 21.6 have SNR $\leqslant$ 12 (40 of the 50 have SNR $\leqslant$ 8), so their non-detection on Aug. 19.6 is in general not surprising. (The 10 with SNRs between 8 and 12 are expected to be detectable with SNRs between ~5 and 7 on Aug. 19.6 assuming the lines were of equal intrinsic strength on both dates.) The 13 unknown emission features that were covered on both dates but detected only on Aug. 19.6 are less convincingly real since they were not seen on Aug. 21.6 (with more on-source time) and all have SNR $\leqslant$ 6.4. For these reasons, these emissions are regarded as possibly spurious and are labeled as (unknown?) in Table 3.

Most of the strong unidentified lines fall between 3300 and 3470 cm^{-1}, a region with a large number of H_2O hot-band lines. As discussed in Section 3.1, some emissions labeled as water blended with an unknown may in fact be pure H_2O, since in some cases there may be a mismatch between observed and expected relative H_2O line intensities. Generally, weaker unidentified features fall between 3060 and 3260 cm^{-1}, where emissions from radicals (mostly OH and NH_2) dominate the identified features. In the region 2702–3060 cm^{-1}, unidentified emissions are fewer, however, there is a prominent unidentified feature near 3040.3 cm^{-1}. We note that many features in this region were assigned to CH_3OH due to wavelength matches but lacking a reliable fluorescence model it is not known if the observed relative line intensities are reasonable. Other organic species are likely present in this region, however, assessing their contributions (or even presence) is impossible at this time due to spectral confusion. Higher spectral resolving power would alleviate this to some extent, but will also likely reveal additional confusion in cases of very closely blended lines (see below).

4. Discussion

4.1. Using spectral surveys to assess the overall volatile chemistry in comets

The first step in the quantitative analysis of these comet data is identifying emission features within spectra and determining contributions (if any) from blends (whether due to single or multiple species). In addition to an overview of the volatile chemistry, this provides a guide to the specific spectral emissions that can be used for extracting quantitative information (e.g., production rates, relative abundances, rotational temperatures, and nuclear spin temperatures), and those that should not be used or need blends modeled out.

Within this spectral survey, we have definitively detected nine molecules (including radicals) that provide important information on the volatile chemistry of Comet Lee: H_2O, C_2H_2, C_2H_6, CH_4, HCN, CH_3OH, H_2CO, OH, and NH_2. Quantitative results from some data within this survey have been published elsewhere (Mumma et al., 2001a; Gibb et al., 2003; Bonev et al., 2004; Dello Russo et al., 2005; DiSanti et al., in prepa-

ration; see also Table 7). Many emission features (18.5%) are unidentified, suggesting that additional species may also be represented in our spectra. We have also noted the many blended emissions and their possible components. The strengths of contributing species need to be established before any quantitative analysis can be performed on blended emissions (e.g., C_2H_6 $^RQ_3$, CH_4 P3). In addition to insights gained on the chemistry of Comet Lee from the inventory of molecular emissions seen in this survey, these spectra provide a standard with which spectra of future comets (or spectra from existing datasets) can be compared. It can also be a valuable tool for planning future high-resolution infrared observations of comets or other objects of astrophysical interest.

4.2. The importance of fluorescence models for interpreting cometary spectra

Lacking fluorescence models, molecular line positions can be noted but determination of molecular abundances is not possible. Fluorescence models are also needed to determine whether flux from an emission is consistent with a single line or due to a blend (e.g., see Section 3.10). To extract quantitative information from comet spectra we developed temperature-dependent fluorescence models for both linear (e.g., HCN, C_2H_2) and non-linear molecules (e.g., H_2O, H_2CO, NH_3, CH_4, and C_2H_6) (cf. Reuter et al., 1989; Dello Russo et al., 2000, 2001; Gibb et al., 2003; DiSanti et al., 2004; Magee-Sauer et al., 2004). Fluorescence models of relevance to comets at infrared wavelengths have also been developed independently for C_2H_6, CH_4 and CH_3D (Kim, 2003; Kawakita et al., 2005). For the determination of line assignments in this work, we compared relative line intensities in these spectra to those predicted from available fluorescence models. If an emission line was significantly weaker than expected we assumed it was due to inaccuracies in the fluorescence model. If an emission line was significantly stronger than expected we assumed that the emission was blended, although this could also be caused by inaccuracies in the fluorescence model. We invoked these assumptions when determining molecular assignments (Tables 3, 4).

Once a fluorescence model is available and assignments have been made, an important consideration is often overlooked when determining quantitative information (e.g., production rates, relative abundances, rotational temperatures and spin temperatures). Errors in these quantities are generally not dominated by the "photon" noise (reflected by the SNR of individual spectral lines), but by line-by-line deviations between the best-fit fluorescence model and the data. The accuracy of a fluorescence model is limited by assumptions made to simplify the model (e.g., a Boltzmann distribution for the initial ground-state population) and/or poorly constrained parameters that can cause either systematic (e.g., uncertainties in band strengths) or non-systematic (e.g., uncertainties in rotational branching ratios) errors (cf. Dello Russo et al., 2004, 2005; Bonev, 2005). Other factors such as unrecognized blends, and errors in the parameters used to generate the best-fit normalized synthetic atmospheric model can also cause errors distinct from the photon noise. Thus, these effects (not photon noise) generally limit the extent to which quantitative data can be constrained (Dello Russo et al., 2004, 2005; Bonev, 2005). For example, errors in the water production rate should reflect the level of agreement between independent measurements of each detected water line. Also, the effects of small sample size should be incorporated when necessary; for example, when a production rate, rotational temperature or spin temperature is determined on the basis of only a few detected emission lines, the error bars should reflect the effects of small number statistics (cf. Bonev, 2005).

As more comets are observed, lines that have systematically deviant predicted intensities can be identified and the fluorescence models corrected. In this way, comets themselves can be used as laboratories to help improve fluorescence models and partially compensate for the paucity of relevant low-temperature laboratory spectra.

4.3. Using high-resolution survey data to help interpret low-resolution infrared data

High-resolution infrared survey spectra can be used to help interpret lower resolution data. One example is determining specific molecular contributors to the 3.2–3.6 μm X–CH feature seen in many comets observed over the last twenty years at low ($\lambda/\Delta\lambda \sim 100$) and moderate ($\lambda/\Delta\lambda \sim 1000$) spectral resolving power (cf. Brooke et al., 1991b; Bockelée-Morvan et al., 1995). The detection of methanol (CH_3OH) in Comet C/1989 X1 Austin (Hoban et al., 1991; Bockelée-Morvan et al., 1991) and the subsequent modeling of its ν_2, ν_3, and ν_9 bands (Reuter, 1992) showed that CH_3OH emission from fundamental bands could contribute some (but not all) of the integrated flux measured in the X–CH feature (see also Davies et al., 1993). A volatile source for this "excess" emission in comets was supported by the observed heliocentric dependence of this feature, which agreed with that of the modeled CH_3OH emission but not with that of dust (DiSanti et al., 1995; Bockelée-Morvan et al., 1995). However, it was apparent that higher spectral resolving power was needed to help identify other volatile species that contribute to the X–CH feature.

In addition to its high-resolution mode, NIRSPEC can obtain spectra of the entire L-band with moderate resolving power ($\lambda/\Delta\lambda \sim 2000$) allowing direct comparison with high-resolution data (Fig. 5). A moderate-resolution spectrum of Comet Lee in the L-band was obtained on UT 1999 Aug. 20.6. This spectrum shows emission present between 3.2 and 3.6 μm, however only CH_3OH (the ν_3 band near 3.52 μm) can be definitively identified (Fig. 5A). The high-resolution survey data enables the determination of other contributing species to the moderate resolution spectrum (Fig. 3). It is also apparent from the high-resolution data that CH_3OH combination and overtone bands, not considered when the X–CH feature was previously modeled (Reuter, 1992), contribute flux to this spectral region (see Section 3.10). Based on the high-resolution survey data, emissions from additional volatile species (including emission from previously unaccounted for CH_3OH bands) contribute significantly to the excess flux seen after subtracting the modeled CH_3OH contribution from low- and moderate-resolution comet

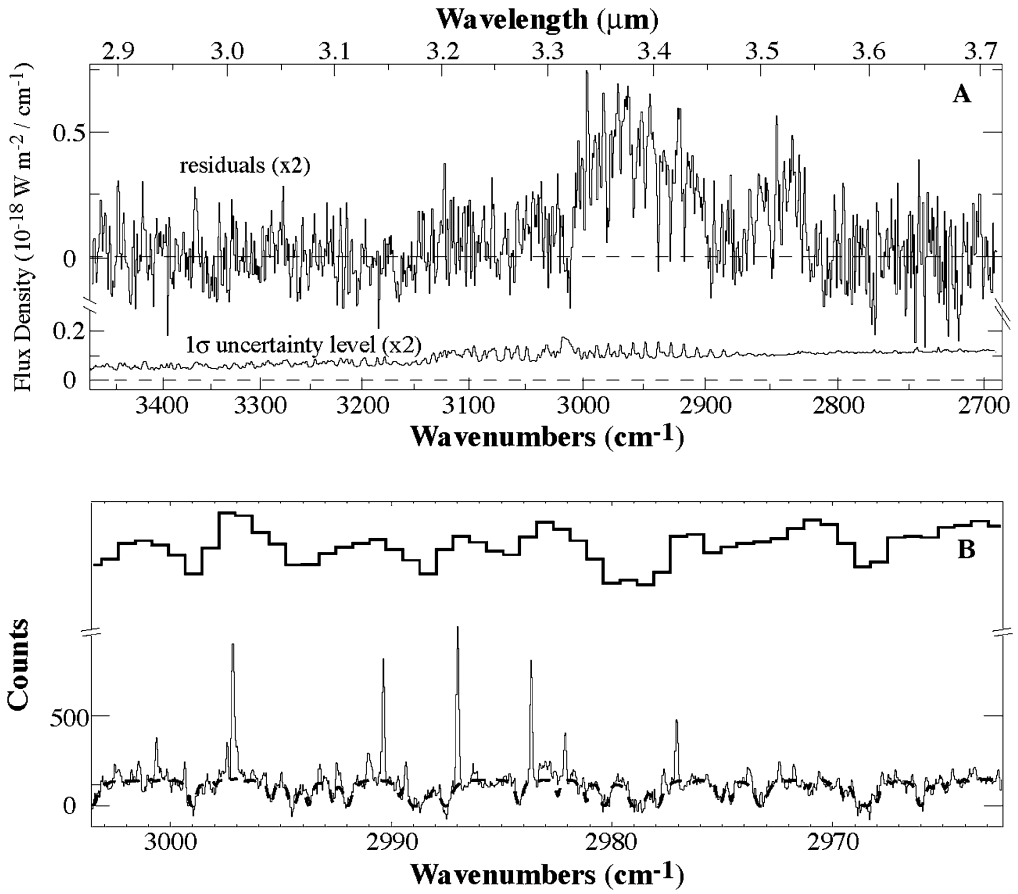

Fig. 5. Spectra of Comet Lee taken in the moderate-dispersion ($\lambda/\Delta\lambda \sim 2000$) mode on UT 1999 August 20.6, and high-dispersion ($\lambda/\Delta\lambda \sim 25{,}000$) mode on August 21.6. (A) Moderate-dispersion spectrum of Comet Lee. The broad feature centered at 3.52 μm is due primarily to CH_3OH ν_3; the broad feature between 3.3–3.45 μm is the X–CH feature (emission primarily from CH_3OH and C_2H_6 with minor contributions from other species; see Section 4.3). The grasp of this spectrum is roughly the same as the spectral coverage obtained in this high-resolution survey (Figs. 2, 3). The estimated channel-by-channel noise (1σ) is shown below (from Mumma et al., 2001a, Fig. 1e). (B) High-dispersion spectrum (lower solid trace) of Comet Lee showing ro-vibrational emission lines from CH_3OH, C_2H_6, CH_4, and OH. A synthetic spectrum of the atmospheric transmittance is also shown (dashed trace). Above (upper solid trace), the moderate-dispersion spectrum in this region is shown for comparison (from Mumma et al., 2001a, Fig. 2c). Individual species cannot be uniquely identified at lower spectral resolving power, demonstrating the significant reduction in spectral confusion realized with higher resolving powers.

data (cf. Reuter, 1992; Davies et al., 1993; DiSanti et al., 1995; Bockelée-Morvan et al., 1995).

Although spectral confusion is not eliminated at the resolving power realized in this survey ($\lambda/\Delta\lambda \sim 25{,}000$), it is clear that high-resolving power is necessary for interpreting the volatile chemistry of comets at infrared wavelengths. High-resolution infrared data show that C_2H_6 has strong emissions that contribute to the X–CH feature (cf. Dello Russo et al., 2001). Based on published band strengths for CH_3OH and C_2H_6, their relative contributions to the X–CH feature can be approximated assuming that atmospheric extinction will affect both species to a similar extent. At 1 AU from the Sun, the combined g-factors for fundamental bands of CH_3OH and C_2H_6 in this region are $\sim 7 \times 10^{-4}$ and 9×10^{-4} s^{-1}, respectively (including the ν_2, ν_9, and ν_3 bands of methanol, Rogers, 1980; including the ν_5 and ν_7 bands of ethane, Dang-Nhu et al., 1984). Accounting for band strengths (fundamental bands only) and production rates derived for these species (Table 7), the relative contributions to the X–CH feature are $(C_2H_6)/(CH_3OH) \sim 0.6$. Comet Lee has a fairly typical C_2H_6/CH_3OH ratio (cf. Mumma et al., 2003), so C_2H_6 is expected to be a major contributor to the X–CH feature in many comets.

Additional volatile species can also contribute flux to the X–CH feature, but their contributions are generally minor compared to CH_3OH and C_2H_6. Although CH_4 is generally abundant in comets and its ν_3 band (near 3.3 μm) is strong, its contribution to the X–CH feature seen in ground-based low-resolution spectra of comets is severely limited by atmospheric extinction (dependent on Δ_{dot}), so in general its importance does not rival CH_3OH and C_2H_6. OH prompt emission could provide a small contribution in discrete regions between 3.0 and 3.6 μm where its multiplets are present, however its contribution to the overall X–CH feature is limited by the moderate strength and relatively small number of OH lines in this region. The ν_1 and ν_5 bands of H_2CO could contribute flux in the 3.45–3.6 μm region, however two factors make the H_2CO contribution in this region typically minor relative to CH_3OH ν_3: (1) H_2CO is generally on the order of several times less abundant than CH_3OH in comets (see Fig. 3 in Biver et al., 2002), and (2) in many comets there is likely a significant or dominant distributed source for H_2CO, so less of the total abundance of H_2CO

Table 8
An example of some undetected molecules in our Comet Lee survey data

Molecule[a]	Positions for emissions (μm)[b]	Factors limiting detectability[c]	Comments
HCOOH	3.40	4, 5, 6	Has been detected in the radio in Hale–Bopp[d]
CH_3CN	3.32, 3.39	1, 4, 5, 6	Has been detected in the radio in comets[d]
C_2H_4	3.22, 3.35	1, 2, 4, 5	Abundance ratio with C_2H_2 and C_2H_6 can establish importance of H-atom addition reactions. Only detectable at IR wavelengths
C_3H_8	3.37, 3.46	2, 4, 5, 6	Next in the homologous saturated hydrocarbon series after CH_4 and C_2H_6
C_2H_5OH	3.37, 3.45	1, 4, 5, 6	Next in the homologous alcohol series after CH_3OH. Also detectable at radio wavelengths
HC_3N	3.01	1, 2, 4	Has been detected in the radio in Hale–Bopp[d]
CH_3CCH	3.00, 3.40	1, 2, 4, 5	A possible parent of C_3[e]
C_4H_2	3.00	1, 2, 4	Only detectable at IR wavelengths
c-C_3H_6	3.22, 3.31	1, 2, 5	
H_2CCO	3.16, 3.26	1, 2, 5	Also detectable at radio wavelengths
HDO	3.70	1	Has been detected in Comets Halley (in situ), Hyakutake (radio), and Hale–Bopp (radio)[f]
DCN	3.80	1	Has been detected in comet Hale–Bopp (radio)[g]
CH_3D	3.31	1, 2, 4	CH_3D/CH_4 abundances 0.1 or higher?[h]
H_2O^+	∼2.87–3.2	2, 3, 4, 5	Detected in comets at visible wavelengths[i]
H_3O^+	∼2.87–3.0	2, 3, 4, 5	Detected at radio wavelengths in Hale–Bopp[j]

[a] Positions for bands and lines for these molecules are available from: HCOOH (Notholt et al., 1991; Ito and Nakanaga, 2000); CH_3CN (Cerceau et al., 1985); C_2H_4 (Van Lerberghe et al., 1972; Dang-Nhu et al., 1983; Bach et al., 1998); C_3H_8 (Shimanouchi, 1972); C_2H_5OH (Rogers, 1980); HC_3N (Mallinson and Fayt, 1976); CH_3CCH (Russell et al., 1971; Kerstel et al., 1994); C_4H_2 (Guelachvili et al., 1984); c-C_3H_6 (Merdes et al., 1991; Plíva et al., 1992); H_2CCO (Johns et al., 1972; Duncan et al., 1987; Escribano et al., 1994); HDO (Rothman et al., 1992); DCN (Bartunek and Barker, 1935); CH_3D (Rothman et al., 1992; Kawakita and Watanabe, 2003); H_2O^+ (Dinelli et al., 1988; Weis et al., 1989; Huet et al., 1992); H_3O^+ (Stahn et al., 1987; Ho et al., 1991; Tang and Oka, 1999).

[b] Approximate wavelength (or range) where infrared ro-vibrational lines are expected.

[c] Factors limiting the ability to detect these species are numbered as in the first paragraph in Section 4.4. (1) Line strengths or abundance; (2) atmospheric transmittance; (3) release as a distributed source; (4) spectral confusion; (5) lack of fluorescence models; (6) lack of information on line positions.

[d] Bockelée-Morvan et al. (2000).

[e] Helbert et al. (2005).

[f] Eberhardt et al. (1987b), Bockelée-Morvan et al. (1998), Meier et al. (1998b).

[g] Meier et al. (1998c).

[h] Aikawa and Herbst (1999).

[i] Cf. Wehinger and Wyckoff (1974).

[j] Lis et al. (1999).

is included within the field of view of small-aperture spectrometers compared with a predominantly native volatile such as CH_3OH. Many other more complex organics have vibrational bands between 3.2 and 3.6 μm, but abundance constraints suggest they probably provide only minor additional contributions to this feature.

4.4. Limitations of high-resolution infrared spectral data

Certain factors limit the ability to detect species with high-resolution ground-based infrared spectroscopy in the L-band. Here we list six important factors that can limit molecular detections in comets: (1) Line strengths or abundances in comets may be too low to be detected at the sensitivity limit of the spectrometer/telescope combination. (2) Some spectral regions are not observable with ground-based spectroscopy due to obscuration by the terrestrial atmosphere. An important example of this is CO_2, an abundant species in comets that has a very strong band near 4.26 μm, but is completely obscured in ground-based observations by terrestrial CO_2. (3) Nucleus-centered spectral extracts emphasize the near-nucleus environment and are thus not optimal for detecting species released in the coma as distributed sources. (4) Even at $\lambda/\Delta\lambda > 10^4$, individual lines from different species may not be fully resolved in some spectral regions due to spectral confusion. Molecular complexity increases the number of observable spectral lines (with C_2H_6 and CH_3OH having the most complex spectra of species identified in this survey). Therefore, it is often impossible to separate the strong lines of less abundant species (e.g., C_2H_5OH) from the weak lines of a more abundant one (e.g., CH_3OH) without precise knowledge of individual line positions and intensities. (5) A means of addressing the problem of spectral confusion—development of accurate fluorescence models—quickly becomes more difficult with increasing molecular complexity. A fluorescence model is essential for modeling relative intensities expected for individual lines at the very low rotational temperatures typical of cometary comae, and for extrapolating the total band intensity (hence, production rate) from the subset of lines actually measured. (6) For more complex molecules, band positions are often known, but positions and assignments for ro-vibrational lines are unavailable. Table 8 lists some molecules that were not detected in this survey and the factors that hinder their detection.

What future molecular detections in comets are likely at L-band? With present instrumentation, some of the species listed in Table 8 could be detected with a favorable apparition of a very productive comet, however, this happens infrequently. In the near future, more powerful spectrometers and telescopes

could allow routine detection of some of these species in moderately productive comets from the ground. Ground-based spectrometers with large-format array detectors that are capable in a single setting of sampling the entire L-band with higher spectral resolving power ($\lambda/\Delta\lambda \sim 10^5$) will likely be available within the next ten years. Higher resolving power would better separate lines in regions of high spectral confusion (e.g., near 3.0 μm, and from ∼3.3–3.55 μm), and would improve line-to-continuum contrast (and sensitivity). Spectral confusion in the 3.0 μm region is mainly due to species with well known line positions and intensities (e.g., HCN, C_2H_2, NH_3, OH, H_2O), so ground-based instruments with increased sensitivity and resolving power could enable routine detections of several minor species with emissions near 3 μm (e.g., HC_3N, CH_3CCH, and C_4H_2).

Detecting new species in the 3.3–3.55 μm region will continue to be problematic even with better sensitivity and higher spectral resolution. The main source of spectral confusion in this region is CH_3OH, a molecule with a complex spectrum, and one for which an adequate fluorescence model for predicting line-by-line intensities (and in some cases positions) from relevant fundamental, overtone, and combination bands is currently lacking. Unless line positions and intensities for all relevant lines of CH_3OH are known (to a high degree of accuracy), spectral confusion will limit the ability to detect new species in this spectral region (e.g., HCOOH, CH_3CN, C_3H_8, C_2H_5OH), even with instruments that deliver higher resolution and sensitivity.

Increased sensitivity and resolving power at infrared wavelengths could help in determining isotopic ratios in comets. Constraining isotopic ratios can provide important information on physical conditions in the early solar nebula, and can help assess the degree to which comets seeded the Earth with volatile material (cf. Bockelée-Morvan et al., 2004). In situ mass spectroscopy of Halley and radio observations of Hyakutake and Hale–Bopp have allowed HDO/H_2O and DCN/HCN ratios to be determined in these comets (Balsiger et al., 1995; Eberhardt et al., 1995; Bockelée-Morvan et al., 1998; Meier et al., 1998b; Meier et al., 1998c). However, measurements in only three comets do not allow definitive conclusions about the formative histories of comets in general or their role in seeding Earth's oceans (cf. Delsemme, 2000).

To date, deuterated species have not been detected in comets at infrared wavelengths, although several have strong emissions in the L-band (e.g., HDO, DCN, CH_3D, C_2H_5D, HDCO). Detection of HDO, DCN, and CH_3D may be possible in a very bright comet with presently available infrared spectrometers (e.g., NIRSPEC), however their more routine detection from ground-based observatories will depend on the development of spectrometers with higher sensitivity and resolution (Table 8). In addition, spectral confusion may become an additional hindrance to the detection of some deuterated species, especially for weak features. Although infrared spectroscopy will likely not enable the routine detection of deuterated species in comets in the near future, it may help increase the sample size by enabling detection in the occasional bright comet.

A high-resolution infrared spectrometer in space would enable read noise-limited sampling without atmospheric extinction. This would enable the detection of species in regions of high atmospheric extinction when observed from the ground at infrared wavelengths (e.g., CO_2, C_2H_4). However, no such mission is presently approved.

5. Summary

We present a high-resolution spectral survey of Comet C/1999 H1 (Lee) covering (with a few small gaps) the entire L-band region from 2.874–3.701 μm (3479–2702 cm^{-1}). This spectral region contains transitions for many molecules important for characterizing the overall volatile chemistry of comets. Using published line lists and laboratory spectra (e.g., Fig. 4) we identified 444 of the 545 distinct emission features present in these spectra. For all detected emissions, we tabulate rest frequencies, relative intensities, signal-to-noise ratios, and assignments. A complete summary is given in Fig. 3 and Tables 3 and 4 (Fig. 3 and Tables 3 and 4 are displayed in their entirety in electronic Supplementary materials). A summary of detected emissions on each date is given in Tables 5 and 6.

High-resolution ($\lambda/\Delta\lambda \sim 2.5 \times 10^4$) spectroscopy with NIRSPEC has for the first time permitted a line-by-line survey of cometary emission over nearly the entire L-band, encompassing the bands of many important cometary molecules. Select regions within this broad range were targeted by earlier high-resolution searches (cf. Mumma et al., 1996; Brooke et al., 1996). Earlier low- and moderate-resolution studies revealed only general band shapes, continuum slopes, etc., however spectral confusion and generally lower line-to-continuum contrast precluded unambiguous identification of specific molecular emissions (with the exception of the ν_3 band of CH_3OH, centered at 3.516 μm). Spectral confusion remains an important issue for high-resolution data in some spectral regions, and adequate fluorescence models and relevant laboratory data are needed for all contributing species (especially CH_3OH) to fully exploit survey data such as those presented herein. This work provides a comparative database for past and future observations of comets with high-resolution ground-based infrared spectroscopy.

Acknowledgments

This work was supported by the NASA OSS Planetary Atmospheres Program under NAG5-10795, NAG5-12285, and NNG05GA64G to N.D.R., and the Planetary Astronomy Program under RTOP 344-32-51-03 to M.J.M. L.-H.X. wishes to acknowledge partial financial support from the Natural Sciences and Engineering Research Council of Canada. Data presented herein were obtained at the W.M. Keck Observatory, which is operated as a scientific partnership among the California Institute of Technology, the University of California and the National Aeronautics and Space Administration. The Observatory was made possible by the generous financial support of the W.M. Keck Foundation. The authors wish to recognize and acknowledge the very significant cultural role and reverence that the summit of Mauna Kea has always had within the indige-

nous Hawaiian community. We are most fortunate to have the opportunity to conduct observations from this mountain.

Supplementary material

Supplementary data associated with this article can be found on ScienceDirect in the online version, at DOI:10.1016/j.jicarus.2006.04.020.

References

Abrams, M.C., Davis, S.P., Rao, M.L.P., Engleman Jr., R., 1990. Highly excited rotational states of the Meinel system of OH. Astrophys. J. 363, 326–330.

A'Hearn, M.F., Millis, R.L., Schleicher, D.G., Osip, D.J., Birch, P.V., 1995. The ensemble properties of comets: Results from narrowband photometry of 85 comets, 1976–1992. Icarus 118, 223–270.

Aikawa, Y., Herbst, E., 1999. Deuterium fractionation in protoplanetary disks. Astrophys. J. 526, 314–326.

Allen, M., Delitsky, M., Huntress, W., Yung, Y., Ip, W.-H., 1987. Evidence for methane and ammonia in the coma of Comet P/Halley. Astron. Astrophys. 187, 502–512.

Altenhoff, W.J., Batrla, W., Huchtmeier, W.K., Schmidt, J., Stumpff, P., Walmsley, M., 1983. Radio observations of Comet 1983d. Astron. Astrophys. 125, L19–L22.

Altwegg, K., Balsiger, H., Geiss, J., 1994. Abundance and origin of the CH_n^+ ions in the coma of Comet P/Halley. Astron. Astrophys. 290, 318–323.

Amano, T., Bernath, P.F., McKellar, A.R.W., 1982a. Direct observation of the ν_1 and ν_3 fundamental bands of NH_2 by difference frequency laser spectroscopy. J. Mol. Spectrosc. 94, 100–113.

Amano, T., Bernath, P.F., Yamada, C., Endo, Y., Hirota, E., 1982b. Difference frequency laser spectroscopy of the ν_3 band of the CH_3 radical. J. Chem. Phys. 77, 5284–5287.

Andresen, P., Ondrey, G.S., Titze, B., Rothe, E.W., 1984. Nuclear and electron dynamics in the photodissociation of water. J. Chem. Phys. 80, 2548–2569.

Arpigny, C., Zeippen, C.J., Klutz, M., Magain, P., Hutsemekers, D., 1987. On the interpretation of the CH cometary spectrum. In: Proceedings of the International Symposium on the Diversity and Similarity of Comets. ESA, pp. 607–612.

Bach, M., Georges, R., Hepp, M., Herman, M., 1998. Slit-jet Fourier transform infrared spectroscopy in $^{12}C_2H_4$: Cold and hot bands near 3000 cm^{-1}. Chem. Phys. Lett. 294, 533–537.

Ball, J.A., Gottlieb, C.A., Lilley, A.E., Radford, H.E., 1970. Detection of methyl alcohol in Sagittarius. Astrophys. J. 162, L203–L210.

Balsiger, H., Altwegg, K., Geiss, J., 1995. D/H and $^{18}O/^{16}O$ ratio in the hydronium ion and in neutral water from in situ ion measurements in Comet P/Halley. J. Geophys. Res. 100, 5827–5834.

Bartunek, P.F., Barker, E.F., 1935. The infrared absorption spectra of linear molecules carbonyl sulfide and deuterium cyanide. Phys. Rev. 48, 516–521.

Bensch, F., Bergin, E.A., Bockelée-Morvan, D., Melnick, G.J., 2004. Submillimeter wave astronomy satellite monitoring of the postperihelion water production rate of Comet C/1999 T1 (McNaught–Hartley). Astrophys. J. 609, 1164–1169.

Bernath, P.F., 1987. The vibration–rotation emission spectrum of $CH(X^2\Pi)$. J. Chem. Phys. 86, 4838–4842.

Bird, M.K., Huchtmeier, W.K., Gensheimer, P., Wilson, T.L., Janardhan, P., Lemme, C., 1997. Radio detection of ammonia in Comet Hale–Bopp. Astron. Astrophys. 325, L5–L8.

Bird, M.K., Janardhan, P., Wilson, T.L., Huchtmeier, W.K., Gensheimer, P., Lemme, C., 1999. K-band radio observations of Comet Hale–Bopp: Detections of ammonia and (possibly) water. Earth Moon Planets 78, 21–28.

Biver, N., and 22 colleagues, 1999. Long term evolution of the outgassing of Comet Hale–Bopp from radio observations. Earth Moon Planets 78, 5–11.

Biver, N., Bockelée-Morvan, D., Crovisier, J., Colom, P., Henry, F., Moreno, R., Paubert, G., Despois, D., Lis, D.C., 2002. Chemical composition diversity among 24 comets observed at radio wavelengths. Earth Moon Planets 90, 323–333.

Bockelée-Morvan, D., Crovisier, J., 1989. The nature of the 2.8-μm emission feature in cometary spectra. Astron. Astrophys. 216, 278–283.

Bockelée-Morvan, D., Colom, P., Crovisier, J., Despois, D., Paubert, G., 1991. Microwave detection of hydrogen sulfide and methanol in Comet Austin (1989c1). Nature 350, 318–320.

Bockelée-Morvan, D., Crovisier, J., Colom, P., Despois, D., 1994. The rotational lines of methanol in Comets Austin 1990 V and Levy 1990 XX. Astron. Astrophys. 287, 647–665.

Bockelée-Morvan, D., Brooke, T.Y., Crovisier, J., 1995. On the origin of the 3.2- to 3.6-μm emission features in comets. Icarus 116, 18–39.

Bockelée-Morvan, D., and 11 colleagues, 1998. Deuterated water in Comet C/1996 B2 (Hyakutake) and its implications for the origin of comets. Icarus 133, 147–162.

Bockelée-Morvan, D., and 17 colleagues, 2000. New molecules found in Comet C/1995 O1 (Hale–Bopp). Investigating the link between cometary and interstellar material. Astron. Astrophys. 353, 1101–1114.

Bockelée-Morvan, D., Crovisier, J., Mumma, M.J., Weaver, H.A., 2004. The composition of cometary volatiles. In: Festou, M.C., Keller, H.U., Weaver, H.A. (Eds.), Comets II. Univ. of Arizona Press, Tucson, pp. 391–423.

Bonev, B.P., 2005. Towards a chemical taxonomy of comets: Infrared spectroscopic methods for quantitative measurements of cometary water (with an independent chapter on Mars polar science). Ph.D. dissertation, Univ. of Toledo. http://astrobiology.gsfc.nasa.gov/Bonev_thesis.pdf.

Bonev, B.P., Mumma, M.J., Dello Russo, N., Gibb, E.L., DiSanti, M.A., Magee-Sauer, K., 2004. Infrared OH prompt emission as a proxy of water production in comets: Quantitative analysis of the multiplet near 3046 cm^{-1} in Comets C/1999 H1 (Lee) and C/2001 A2 (LINEAR). Astrophys. J. 615, 1048–1053.

Boogert, A.C.A., Schutte, W.A., Tielens, A.G.G.M., Whittet, D.C.B., Helmich, F.P., Ehrenfreund, P., Wesselius, P.R., De Graauw, Th., Prusti, T., 1996. Solid methane toward deeply embedded protostars. Astron. Astrophys. 315, L377–L380.

Boogert, A.C.A., Blake, G.A., Oberg, K., 2004. Methane abundance variations toward the massive protostar NGC 7538 IRS 9. Astrophys. J. 615, 344–353.

Brooke, T.Y., Tokunaga, A.T., Weaver, H.A., Chin, G., Geballe, T.R., 1991a. A sensitive upper limit on the methane abundance in Comet Levy (1990c). Astrophys. J. 372, L113–L116.

Brooke, T.Y., Tokunaga, A.T., Knacke, R.F., 1991b. Detection of the 3.4 micron emission feature in Comets P/Brorsen–Metcalf and Okazaki–Levy–Rudenko (1989r) and an observational summary. Astron. J. 101, 268–278.

Brooke, T.Y., Tokunaga, A.T., Weaver, H.A., Crovisier, J., Bockelée-Morvan, D., Crisp, D., 1996. Detection of acetylene in the infrared spectrum of Comet Hyakutake. Nature 383, 606–608.

Brooke, T.Y., Sellgren, K., Geballe, T.R., 1999. New 3 micron spectra of young stellar objects with H_2O ice bands. Astrophys. J. 517, 883–900.

Brooke, T.Y., Weaver, H.A., Chin, G., Bockelée-Morvan, D., Kim, S.J., Xu, L.-H., 2003. Spectroscopy of Comet Hale–Bopp in the infrared. Icarus 166, 167–187.

Carrington, T., 1964. Angular momentum distribution and emission spectrum of OH ($^2\Sigma^+$) in the photodissociation of H_2O. J. Chem. Phys. 41, 2012–2018.

Cerceau, F., Raulin, F., Courtin, R., Gautier, D., 1985. Infrared spectra of gaseous mononitriles: Application to the atmosphere of Titan. Icarus 62, 207–220.

Chiu, K., Neufeld, D.A., Bergin, E.A., Melnick, G.J., Patten, B.M., Wang, Z., Bockelée-Morvan, D., 2001. Postperihelion SWAS observations of water vapor in the coma of Comet C/1999 H1 (Lee). Icarus 154, 345–349.

Combes, M., and 18 colleagues, 1986. Infrared sounding of Comet Halley from Vega 1. Nature 321, 266–268.

Combes, M., and 16 colleagues, 1988. The 2.5–12 μm spectrum of Comet Halley from the IKS-VEGA experiment. Icarus 76, 404–436.

Combi, M.R., Delsemme, A.H., 1986. Neutral cometary atmospheres. V. C_2 and CN in comets. Astrophys. J. 308, 472–484.

Combi, M.R., Fink, U., 1997. A critical study of molecular photodissociation and CHON grain sources for cometary C_2. Astrophys. J. 484, 879–890.

Cottin, H., Bénilan, Y., Gazeau, M.-C., Raulin, F., 2004. Origin of cometary extended sources from degradation of refractory organics on grains: Polyoxymethylene as formaldehyde parent molecule. Icarus 167, 397–416.

Crovisier, J., 1987. Synthetic spectra of linear parent molecules in comets. Astron. Astrophys. 68 (Suppl.), 223–258.

Crovisier, J., 1989. The photodestruction of water in cometary atmospheres. Astron. Astrophys. 213, 459–464.

Crovisier, J., 1998. Physics and Chemistry of comets: Recent results from Comets Hyakutake and Hale–Bopp. Faraday Discuss. 109, 437–452.

Crovisier, J., Leech, K., Bockelée-Morvan, D., Brooke, T.Y., Hanner, M.S., Altieri, B., Keller, H.U., Lellouch, E., 1997. The spectrum of Comet Hale–Bopp (C/1995 O1) observed with the Infrared Space Observatory at 2.9 astronomical units from the Sun. Science 275, 1904–1907.

Crovisier, J., Colom, P., Gérard, E., Bockelée-Morvan, D., Bourgois, G., 2002. Observations at Nançay of the OH 18-cm lines in comets: The data base Observations made from 1982 to 1999. Astron. Astrophys. 393, 1053–1064.

Dang-Nhu, M., Pine, A.S., Robiette, A.G., 1979. Spectral intensities in the ν_3 bands of $^{12}CH_4$ and $^{13}CH_4$. J. Mol. Spectrosc. 77, 57–68.

Dang-Nhu, M., Pine, A.S., Fayt, A., De Vleeschouwer, M., Lambeau, C., 1983. Les intensités dans la pentade ν_{11}, $\nu_2+\nu_{12}$, $2\nu_{10}+\nu_{12}$, ν_9 et $\nu_3+\nu_8+\nu_{10}$ de $^{12}C_2H_4$. Can. J. Phys. 61, 514–521.

Dang-Nhu, M., Pine, A.S., Lafferty, W.J., 1984. Les intensités dans les bandes ν_5, ν_7 et $\nu_8+\nu_1 1$ de l'ethane $^{12}C_2H_6$. Can. J. Phys. 62, 512–519.

Dartois, E., Schutte, W., Geballe, T.R., Demyk, K., Ehrenfreund, P., D'Hendecourt, L., 1999. Methanol: The second most abundant ice species toward the high-mass protostars RAFGL70095 and W33A. Astron. Astrophys. 342, L32–L35.

Davies, J.K., Mumma, M.J., Reuter, D.C., Hoban, S., Weaver, H.A., Puxley, P.J., Lumsden, S.L., 1993. The infrared (3.2–3.6 μm) spectrum of Comet P/Swift-Tuttle: Detection of methanol and other organics. Mon. Not. R. Astron. Soc. 265, 1022–1026.

Dello Russo, N., DiSanti, M.A., Mumma, M.J., Magee-Sauer, K., Rettig, T.W., 1998. Carbonyl sulfide in Comets C/1996 B2 (Hyakutake) and C/1995 O1 (Hale–Bopp): Evidence for an extended source in Hale–Bopp. Icarus 135, 377–388.

Dello Russo, N., Mumma, M.J., DiSanti, M.A., Magee-Sauer, K., Novak, R., Rettig, T.W., 2000. Water production and release in Comet C/1995 O1 Hale–Bopp. Icarus 143, 324–337.

Dello Russo, N., Mumma, M.J., DiSanti, M.A., Magee-Sauer, K., Novak, R., 2001. Ethane production and release in Comet C/1995 O1 Hale–Bopp. Icarus 153, 162–179.

Dello Russo, N., Mumma, M.J., DiSanti, M.A., Magee-Sauer, K., 2002a. Production of ethane and water in Comet C/1996 B2 Hyakutake. J. Geophys. Res. Planets 107 (E11), doi:10.1029/2001JE001838. 5095.

Dello Russo, N., DiSanti, M.A., Magee-Sauer, K., Gibb, E., Mumma, M.J., 2002b. Production of C_2H_6 and H_2O in Comet 2002 C1 Ikeya–Zhang on one date. In: Proceedings of the Asteroids, Comets, Meteors Conference, Berlin, Germany, 2002. ESA SP-500, pp. 689–692.

Dello Russo, N., DiSanti, M.A., Magee-Sauer, K., Gibb, E.L., Mumma, M.J., Barber, R.J., Tennyson, J., 2004. Water production and release in Comet 153P/Ikeya–Zhang (C/2002 C1): Accurate rotational temperature retrievals from hot-band lines near 2.9-μm. Icarus 168, 186–200.

Dello Russo, N., Bonev, B.P., DiSanti, M.A., Mumma, M.J., Gibb, E.L., Magee-Sauer, K., Barber, R.J., Tennyson, J., 2005. Water production rates, rotational temperatures, and spin temperatures in Comets C/1999 H1 (Lee), C/1999 S4, and C/2001 A2. Astrophys. J. 621, 537–544.

Delsemme, A.H., 2000. Cometary origin of the biosphere. Icarus 146, 313–325.

Despois, D., Crovisier, J., Bockelée-Morvan, D., Schraml, J., Forveille, T., Gerard, E., 1986. Observations of hydrogen cyanide in Comet Halley. Astron. Astrophys. 160, L11–L12.

Dinelli, B.M., Crofton, M.W., Oka, T., 1988. Infrared spectroscopy of the ν_3 band of H_2O^+. J. Mol. Spectrosc. 127, 1–11.

DiSanti, M.A., Mumma, M.J., Geballe, T.R., Davies, J.K., 1995. Systematic observations of methanol and other organics in Comet P/Swift–Tuttle: Discovery of new spectral structure at 3.42 μm. Icarus 116, 1–17.

DiSanti, M.A., Dello Russo, N., Magee-Sauer, K., Gibb, E.L., Reuter, D.C., Mumma, M.J., 2002. CO, H_2CO, and CH_3OH in Comet C/2002 C1 Ikeya–Zhang. In: Proceedings of the Asteroids, Comets, Meteors Conference, Berlin, Germany, 2002. ESA SP-500, pp. 571–574.

DiSanti, M.A., Reuter, D.C., Mumma, M.J., Dello Russo, N., Magee-Sauer, K., Gibb, E.L., Bonev, B., Anderson, W.M., 2004. Modeling formaldehyde ν_1 and ν_5 band emission in Comet C/2002 T7 (LINEAR). Bull. Am. Astron. Soc. 36, 1122.

DiSanti, M.A., Bonev, B.P., Magee-Sauer, K., Dello Russo, N., Mumma, M.J., Reuter, D.C., Villanueva, G.L., 2006. Detection of formaldehyde emission in Comet C/2002 T7 (LINEAR) at infrared wavelengths: Line-by-line validation of modeled fluorescent intensities. Astrophys. J. In press.

Drapatz, S., Larson, H.P., Davis, D.S., 1987. Search for methane in Comet P/Halley. Astron. Astrophys. 187, 497–501.

Duncan, J.L., Ferguson, A.M., Harper, J., Tonge, K.H., Hegelund, F., 1987. High-resolution infrared ro-vibrational studies of the A_1 species fundamentals of isotopic ketenes. J. Mol. Spectrosc. 122, 72–93.

Eberhardt, P., 1999. Comet Halley's gas composition and extended sources: Results from the neutral mass spectrometer on Giotto. Space Sci. Rev. 90, 45–52.

Eberhardt, P., and 11 colleagues, 1987a. The CO and N_2 abundance in Comet P/Halley. Astron. Astrophys. 187, 481–484.

Eberhardt, P., Dolder, U., Schulte, W., Krankowsky, D., Lämmerzahl, P., Hoffman, J.H., Hodges, R.R., Berthelier, J.J., Illiano, J.M., 1987b. The D/H ratio in water from Comet P/Halley. Astron. Astrophys. 187, 435–437.

Eberhardt, P., Reber, M., Krankowsky, D., Hodges, R.R., 1995. The D/H and $^{18}O/^{16}O$ ratios in water from Comet P/Halley. Astron. Astrophys. 302, 301–316.

Engel, V., Schinke, R., Staemmler, V., 1988. Photodissociation dynamics of H_2O and D_2O in the first absorption band: A complete ab initio treatment. J. Chem. Phys. 88, 129–148.

Escribano, R., Doménech, J.L., Cancio, P., Ortigoso, J., Santos, J., Bermejo, D., 1994. The ν_1 band of ketene. J. Chem. Phys. 101, 937–949.

Féjard, L., Champion, J.P., Jouvard, J.M., Brown, L.R., Pine, A.S., 2000. The intensities of methane in the 3–5 μm region revisited. J. Mol. Spectrosc. 201, 83–94.

Feldman, P.D., 1983. Ultraviolet spectroscopy and the composition of cometary ice. Science 219, 347–354.

Feldman, P.D., Cochran, A., Combi, M.R., 2005. Spectroscopic investigations of fragment species in the coma. In: Festou, M.C., Keller, H.U., Weaver, H.A. (Eds.), Comets II. Univ. of Arizona Press, Tucson, pp. 425–447.

Fink, U., Hicks, M.D., 1996. A survey of 39 comets using CCD spectroscopy. Astrophys. J. 459, 729–743.

Fray, N., Bénilan, Y., Cottin, H., Gazeau, M.-C., Crovisier, J., 2005. The origin of the CN radical in comets: A review from observations and models. Planet. Space Sci. 53, 1243–1262.

Ghérissi, S., Henry, A., Loete, M., Valentin, A., 1981. Transition moment and line strengths of the ν_3 band of $^{12}CH_4$. J. Mol. Spectrosc. 86, 344–356.

Gibb, E.L., Mumma, M.J., Dello Russo, N., DiSanti, M.A., Magee-Sauer, K., 2003. Methane in Oort cloud comets. Icarus 165, 391–406.

Greenberg, J.M., Hage, J.I., 1990. From interstellar dust to comets: A unification of observational constraints. Astrophys. J. 361, 260–274.

Greene, T.P., Tokunaga, A.T., Toomey, D.W., Carr, J.B., 1993. CSHELL: A high spectral resolution 1–5 μm cryogenic echelle spectrograph for the IRTF. Proc. SPIE 1946, 313–324.

Guelachvili, G., Craig, A.M., Ramsay, D.A., 1984. High-resolution Fourier studies of diacetylene in the regions of the ν_4 and ν_5 fundamentals. J. Mol. Spectrosc. 105, 156–192.

Hausler, D., Andresen, P., Schinke, R., 1987. State to state photodissociation of H_2O in the first absorption band. J. Chem. Phys. 87, 3949–3965.

Helbert, J., Rauer, H., Boice, D.C., Huebner, W.F., 2005. The chemistry of C_2 and C_3 in the coma of Comet C/1995 O1 (Hale–Bopp) at heliocentric distances $r_h \geqslant 2.9$ AU. Astron. Astrophys. 442, 1107–1120.

Hiraoka, K., Takayama, T., Euchi, A., Handa, H., Sato, T., 2000. Study of the reactions of H and D atoms with solid C_2H_2, C_2H_4, and C_2H_6 at cryogenic temperatures. Astrophys. J. 532, 1029–1037.

Hirota, T., Yamamoto, S., Kawaguchi, K., Sakamoto, A., Ukita, N., 1999. Observations of HCN, HNC, and NH_3 in Comet Hale–Bopp. Astrophys. J. 520, 895–900.

Ho, W.C., Pursell, C.J., Oka, T., 1991. Infrared spectroscopy in an H_2–O_2–He discharge: H_3O^+. J. Mol. Spectrosc. 149, 530–541.

Hoban, S., Mumma, M.J., Reuter, D.C., DiSanti, M., Joyce, R.R., 1991. A tentative identification of methanol as the progenitor of the 3.52-μm emission feature in several comets. Icarus 93, 122–134.

Hoban, S., Reuter, D.C., DiSanti, M.A., Mumma, M.J., Elston, R., 1993. Infrared observations of methanol in Comet P/Swift–Tuttle. Icarus 105, 548–556.

Huet, T.R., Pursell, C.J., Ho, W.C., Dinelli, B.M., Oka, T., 1992. Infrared spectroscopy and equilibrium structure of H_2O^+ (X^2B_1). J. Chem. Phys. 97, 5977–5987.

Hunt, R.H., Shelton, W.N., Cook, W.B., Bignall, O.N., Mirick, J.W., Flaherty, F.A., 1991. Torsion–rotation absorption line assignments in the symmetric CH-stretch fundamental of methanol. J. Mol. Spectrosc. 149, 252–256.

Ito, F., Nakanaga, T., 2000. A jet-cooled infrared spectrum of the formic acid dimer by cavity ring-down spectroscopy. Chem. Phys. Lett. 318, 571–577.

Jensen, P., 1988. Calculation of rotation–vibration linestrengths for triatomic molecules using a variational approach: Application to the fundamental bands of CH_2. J. Mol. Spectrosc. 132, 429–457.

Johns, J.W.C., Stone, J.M.R., Winnewisser, G., 1972. The ground state of ketene. J. Mol. Spectrosc. 42, 523–535.

Kaiser, R.I., Balucani, N., 2002. Astrobiology—The final frontier in chemical reaction dynamics. Int. J. Astrobiol. 1, 15–23.

Kawakita, H., and 18 colleagues, 2001. The spin temperature of NH_3 in Comet C/1999 S4 (LINEAR). Science 294, 1089–1091.

Kawakita, H., Watanabe, J., Fuse, T., Furusho, R., Abe, S., 2002. Spin temperature of ammonia determined from NH_2 in Comet C/2001 A2 (LINEAR). Earth Moon Planets 90, 371–379.

Kawakita, H., Watanabe, J., 2003. Fluorescence efficiencies of monodeuteriomethane in comets: Toward the determination of D/H ratio in methane. Astrophys. J. 582, 534–539.

Kawakita, H., Watanabe, J., Kinoshita, D., Ishiguro, M., Nakamura, R., 2003. Saturated hydrocarbons in Comet 153P/Ikeya–Zhang: Ethane, methane, and monodeuterio-methane. Astrophys. J. 590, 573–578.

Kawakita, H., Watanabe, J., Furusho, R., Fuse, T., Capria, M.T., De Sanctis, M.C., Cremonese, G., 2004. Spin temperatures of ammonia and water molecules in comets. Astrophys. J. 601, 1152–1158.

Kawakita, H., Watanabe, J., Furusho, R., Fuse, T., Boice, D.C., 2005. Nuclear spin temperature and deuterium-to-hydrogen ratio of methane in Comet C/2001 Q4 (NEAT). Astrophys. J. 623, L49–L52.

Kawara, K., Gregory, B., Yamamoto, T., Shibai, H., 1988. Infrared spectroscopic observation of methane in Comet P/Halley. Astron. Astrophys. 207, 174–181.

Kerstel, E.R.Th., Lehmann, K.K., Pate, B.H., Scoles, G., 1994. Reinvestigation of the acetylenic C–H stretching fundamental of propyne via high resolution, optothermal infrared spectroscopy: Non-resonant perturbations to ν_1. J. Chem. Phys. 100, 2588–2595.

Kim, S.J., 2003. Infrared excitation processes of C_2H_6 in comets. Earth Planets Space 55, 139–151.

Kleiner, I., Brown, L.R., Tarrago, G., Kou, Q.-L., Picqué, N., Guelachvili, G., Dana, V., Mandin, J.-Y., 1999. Positions and intensities in the $2\nu_4/\nu_1/\nu_3$ vibrational system of $^{14}NH_3$ near 3 μm. J. Mol. Spectrosc. 193, 46–71.

Knacke, R.F., Brooke, T.Y., Joyce, R.R., 1986. Observations of 3.2–3.6 micron emission features in Comet Halley. Astrophys. J. 310, L49–L53.

Kunde, V.G., Maguire, J.C., 1974. Direct integration transmittance model. J. Quant. Spectrosc. Radiat. Trans. 14, 803–817.

Lacy, J.H., Carr, J.S., Evans II, N.J., Baas, F., Achtermann, J.M., Arens, J.F., 1991. Discovery of interstellar methane: Observations of gaseous and solid CH_4 absorption toward young stars in molecular clouds. Astrophys. J. 376, 556–560.

Lafferty, W.J., Thibault, R.J., 1964. High-resolution infrared spectra of $C_2{}^{12}H_2$, $C^{12}C^{13}H_2$, and $C_2{}^{13}H_2$. J. Mol. Spectrosc. 14, 79–96.

Larson, H.P., Weaver, H.A., Mumma, M.J., Drapatz, S., 1989. Airborne infrared spectroscopy of Comet Wilson (1986I) and comparisons with Comet Halley. Astrophys. J. 338, 1106–1114.

Lecacheux, A., and 21 colleagues, 2003. Observations of water in comets with Odin. Astron. Astrophys. 402, L55–L58.

Lis, D.C., and 10 colleagues, 1999. New molecular species in Comet C/1995 (Hale–Bopp) observed with the Caltech Submillimeter Observatory. Earth Moon Planets 78, 13–20.

Lovell, A.J., Kallivayalil, N., Schloerb, F.P., Combi, M.R., Hansen, K.C., Gombosi, T.I., 2004. On the effect of electron collisions in the excitation of cometary HCN. Astrophys. J. 613, 615–621.

Magee-Sauer, K., Mumma, M.J., DiSanti, M.A., Dello Russo, N., Rettig, T.W., 1999. Infrared spectroscopy of the ν_3 band of hydrogen cyanide in C/1995 O1 Hale–Bopp. Icarus 142, 498–508.

Magee-Sauer, K., Mumma, M.J., DiSanti, M.A., Dello Russo, N., 2002a. Hydrogen cyanide in Comet C/1996 B2 Hyakutake. J. Geophys. Res. Planets 107 (E11), doi:10.1029/2002JE001863. 5096

Magee-Sauer, K., Dello Russo, N., DiSanti, M.A., Gibb, E., Mumma, M.J., 2002b. Production of HCN and C_2H_2 in Comet C/2002 C1 Ikeya–Zhang on UT April 13.8 2002b. In: Proceedings of the Asteroids, Comets, Meteors Conference, Berlin, Germany, 2002. ESA SP-500, pp. 549–552.

Magee-Sauer, K., Dello Russo, N., DiSanti, M.A., Bonev, B., Gibb, E.L., Mumma, M.J., 2004. HCN, C_2H_2, and NH_3 abundances in Comet C/LINEAR 2002 T7. Bull. Am. Astron. Soc. 36, 1125.

Maillard, J.P., Chauville, J., Mantz, A.W., 1976. High-resolution emission spectrum of OH in an oxyacetylene flame from 3.7 to 0.9 μm. J. Mol. Spectrosc. 63, 120–141.

Mallinson, P.D., Fayt, A., 1976. High-resolution infra-red studies of HCCCN and DCCCN. Mol. Phys. 32, 473–485.

Manfroid, J., Jehin, E., Hutsemékers, D., Cochran, A., Zucconi, J.-M., Arpigny, C., Schulz, R., Stuwe, J.A., 2005. Isotopic abundance of nitrogen and carbon in distant comets. Astron. Astrophys. 432, L5–L8.

McLean, I.A., and 14 colleagues, 1998. The design and development of NIRSPEC: A near-infrared echelle spectrograph for the Keck II telescope. Proc. SPIE 3354, 566–578.

Meier, R., Eberhardt, P., Krankowsky, D., Hodges, R.R., 1994. Ammonia in Comet P/Halley. Astron. Astrophys. 287, 268–278.

Meier, R., Wellnitz, D., Kim, S.J., A'Hearn, M.F., 1998a. The NH and CH bands of Comet C/1996 B2 (Hyakutake). Icarus 136, 268–279.

Meier, R., Owen, T.C., Matthews, H.E., Jewitt, D.C., Bockelée-Morvan, D., Biver, N., Crovisier, J., Gautier, D., 1998b. A determination of the HDO/H_2O ratio in Comet C/1995 O1 (Hale–Bopp). Science 279, 842–844.

Meier, R., Owen, T.C., Jewitt, D.C., Matthews, H.E., Senay, M., Biver, N., Bockelée-Morvan, D., Crovisier, J., Gautier, D., 1998c. Deuterium in Comet C/1995 O1 (Hale–Bopp): Detection of DCN. Science 279, 1707–1710.

Mélen, F., Herman, M., Matti, G.Y., McNaughton, D.M., 1993. Fourier transform jet spectrum of the ν_7 band of C_2H_6. J. Mol. Spectrosc. 160, 601–603.

Merdes, D.W., Plíva, J., Pine, A.S., 1991. Perpendicular bands of cyclopropane in the 3.5 μm region. J. Mol. Spectrosc. 147, 431–447.

Moroz, V.I., and 16 colleagues, 1987. Detection of parent molecules in Comet Halley from the IKS-Vega experiment. Astron. Astrophys. 187, 513–518.

Mumma, M.J., Weaver, H.A., Larson, H.P., Davis, D.S., Williams, M., 1986. Detection of water vapor in Halley's comet. Science 232, 1523–1528.

Mumma, M.J., Reuter, D.C., 1989. On the identification of formaldehyde in Halley's comet. Astrophys. J. 344, 940–948.

Mumma, M.J., DiSanti, M.A., Tokunaga, A., Roettger, E.E., 1995. Ground-based detection of water in Comet Shoemaker–Levy 1992 XIX: Probing cometary parent molecules by hot-band fluorescence. Bull. Am. Astron. Soc. 27, 1144.

Mumma, M.J., DiSanti, M.A., Dello Russo, N., Fomenkova, M., Magee-Sauer, K., Kaminski, C.D., Xie, D.X., 1996. Detection of abundant ethane and methane, along with carbon monoxide and water, in Comet C/1996 B2 Hyakutake: Evidence for interstellar origin. Science 272, 1310–1314.

Mumma, M.J., DiSanti, M.A., Dello Russo, N., Magee-Sauer, K., Rettig, T.W., 2000. Detection of CO and ethane in Comet 21P/Giacobini–Zinner: Evidence for variable chemistry in the outer solar nebula. Astrophys. J. 531, L155–L159.

Mumma, M.J., and 17 colleagues, 2001a. A survey of organic volatile species in Comet C/1999 H1 (Lee) using NIRSPEC at the Keck Observatory. Astrophys. J. 546, 1183–1193.

Mumma, M.J., Dello Russo, N., DiSanti, M., Magee-Sauer, K., Novak, R.E., Brittain, S., Rettig, T., McLean, I.S., Reuter, D.C., 2001b. The startling organic composition of C/1999 S4 (Linear): A comet formed near Jupiter? Science 292, 1334–1339.

Mumma, M.J., DiSanti, M.A., Dello Russo, N., Magee-Sauer, K., Gibb, E., Novak, R., 2003. Remote infrared observations of parent volatiles in comets: A window on the early Solar System. Adv. Space Res. 31, 2563–2575.

Nizkorodov, S.A., Ziemkiewicz, M., Myers, T.L., Nesbitt, D.J., 2003. Vibrationally mediated dissociation dynamics of H_2O in the $\nu_{OH} = 2$ polyad. J. Chem. Phys. 119, 10158–10168.

Notesco, G., Laufer, D., Bar-Nun, A., 1997. The source of the high C_2H_6/CH_4 ratio in Comet Hyakutake. Icarus 125, 471–473.

Notesco, G., Bar-Nun, A., 2005. A ∼25 K temperature of formation for the submicron ice grains which formed comets. Icarus 175, 546–550.

Notholt, J., Cappellani, F., Roesdahl, H., Restelli, G., 1991. Absolute infrared band intensities and air broadening coefficient for spectroscopic measurements of formic acid in air. Spectrochim. Acta 47A, 477–483.

Oro, J., Mills, T., Lazcano, A., 1992. Comets and the formation of biochemical compounds on the primitive Earth—A review. Origins Life 21, 267–277.

Palmer, P., Wootten, A., Butler, B., Bockelée-Morvan, D., Crovisier, J., Despois, D., Yeomans, D.K., 1996. Comet Hyakutake: First secure detection of ammonia in a comet. Bull. Am. Astron. Soc. 28, 927–928.

Pine, A.S., Lafferty, W.J., 1982. Torsional splittings and assignments of the Doppler-limited spectrum of ethane in the C–H stretching region. J. Res. Natl. Bur. Stand. 87, 237–256.

Plíva, J., Merdes, D.W., Pine, A.S., 1992. Parallel bands of cyclopropane in the 3.2-μm region. J. Mol. Spectrosc. 153, 133–144.

Pontoppidan, K.M., Dartois, D., van Dishoeck, E.F., Thi, W.-F., d'Hendecourt, L., 2003. Detection of abundant solid methanol toward young low mass stars. Astron. Astrophys. 404, L17–L20.

Rauer, H., Arpigny, C., Boehnhardt, H., Colas, F., Crovisier, J., Jorda, L., Küppers, M., Manfroid, J., Rembor, K., Thomas, N., 1997. Optical observations of Comet Hale–Bopp (C/1995 O1) at large heliocentric distances before perihelion. Science 275, 1909–1912.

Reuter, D.C., 1992. The contribution of methanol to the 3.4 micron emission feature in comets. Astrophys. J. 386, 330–335.

Reuter, D.C., Mumma, M.J., Nadler, S., 1989. Infrared fluorescence efficiencies for the ν_1 and ν_5 bands of formaldehyde in the solar radiation field. Astrophys. J. 341, 1045–1058.

Roche, A.E., Wells, W.C., Cosmovici, C.B., Drapatz, S., Michel, K.W., 1975. An upper limit for methane production from Comet Kohoutek by high-resolution tilting-filter photometry at 3.3-micron. Icarus 24, 120–127.

Rogers, D. J., 1980. Infrared intensities of alcohols and ethers. Ph.D. dissertation, Univ. of Florida.

Rothman, L.S., and 13 colleagues, 1992. The HITRAN molecular database: Editions of 1991 and 1992. J. Quant. Spectrosc. Radiat. Trans. 48, 469–507.

Russell, J.W., Murphy, M., Faulkner, T.R., Sugai, S., 1971. High-resolution spectra of ν_1 of CH_3CCH. Spectrochim. Acta 27A, 119–123.

Schleicher, D.G., A'Hearn, M.F., 1982. OH fluorescence in comets: Fluorescence efficiency of the ultraviolet bands. Astrophys. J. 258, 864–877.

Schloerb, F.P., Kinzel, W.M., Swade, D.A., Irvine, W.M., 1986. HCN production from Comet Halley. Astrophys. J. 310, L55–L60.

Shimanouchi, T., 1972. Tables of molecular vibrational frequencies, Consolidated volume I. Nat. Stand. Ref. Data Ser. 39, 1–160.

Sorkhabi, O., Blunt, V.M., Lin, H., A'Hearn, M.F., Weaver, H.A., Arpigny, C., Jackson, W.M., 1997. Using photochemistry to explain the formation and observation of C_2 in comets. Planet. Space Sci. 45, 721–730.

Stahn, A., Solka, H., Adams, H., Urban, W., 1987. The ν_3 band of the molecular ion H_3O^+. Mol. Phys. 60, 121–128.

Swings, P., Elvey, C.T., Babcock, H.W., 1941. The spectrum of Comet Cunningham, 1940c. Astrophys J. 94, 320–343.

Tang, J., Oka, T., 1999. Infrared spectroscopy of H_3O^+: The ν_1 fundamental band. J. Mol. Spectrosc. 196, 120–130.

Tennyson, J., Zobov, N.F., Williamson, R., Polyansky, O.L., Bernath, P.F., 2001. Experimental energy levels of the water molecule. J. Phys. Chem. Ref. Data 30, 735–831.

Tokunaga, A.T., Toomey, D.W., Carr, J., Hall, D.N.B., Epps, H.W., 1990. Design for a 1–5-micron cryogenic echelle spectrograph for the NASA IRTF. Proc. SPIE 1235, 131–143.

Vander Auwera, J., Hurtmans, D., Carleer, M., Herman, M., 1993. The ν_3 fundamental in C_2H_2. J. Mol. Spectrosc. 157, 337–357.

Van Lerberghe, D., Wright, I.J., Duncan, J.L., 1972. High-resolution infrared spectrum and rotational constants of ethylene-H_4. J. Mol. Spectrosc. 42, 251–273.

Veal, J.M., Snyder, L.E., Wright, M., Woodney, L.M., Palmer, P., Forster, J.R., de Pater, I., A'Hearn, M.F., Kuan, Y.-J., 2000. An interferometric study of HCN in Comet Hale–Bopp (C/1995 O1). Astron. J. 119, 1498–1511.

Weaver, H.A., Mumma, M.J., 1984. Infrared molecular emissions from comets. Astrophys. J. 276, 782–797.

Weaver, H.A., Brooke, T.Y., Chin, G., Kim, S.J., Bockelée-Morvan, D., Davies, J.K., 1999a. Infrared spectroscopy of Comet Hale–Bopp. Earth Moon Planets 78, 71–80.

Weaver, H.A., Chin, G., Bockelée-Morvan, D., Crovisier, J., Brooke, T.Y., Cruikshank, D.P., Geballe, T.R., Kim, S.J., Meier, R., 1999b. An infrared investigation of volatiles in Comet 21P/Giacobini–Zinner. Icarus 142, 482–497.

Wehinger, P., Wyckoff, S., 1974. H_2O^+ in spectra of Comet Bradfield (1974b). Astrophys. J. 192, L41–L42.

Weis, B., Carter, S., Rosmus, P., Werner, H.-J., Knowles, P.J., 1989. A theoretical rotationally resolved infrared spectrum for H_2O^+ (X^2B_1). J. Chem. Phys. 91, 2818–2833.

Wink, J., and 10 colleagues, 1999. Evidences for extended sources and temporal modulations in molecular observations of C/1995 O1 (Hale–Bopp) at the IRAM interferometer. Earth Moon Planets 78, 63.

Wright, M.C.H., and 10 colleagues, 1998. Mosaiced images and spectra of $J = 1 \leftarrow 0$ HCN and HCO^+ emission from Comet Hale–Bopp (1995 O1). Astron. J. 116, 3018–3028.

Wyckoff, S., Tegler, S., Wehinger, P.A., Spinrad, H., Belton, M.J.S., 1988. Abundances in Comet Halley at the time of the spacecraft encounters. Astrophys. J. 325, 927–938.

Wyckoff, S.W., Tegler, S.C., Engel, L., 1991. Nitrogen abundance in Comet Halley. Astrophys. J. 367, 641–648.

Xu, L.-H., Wang, X., Cronin, T.J., Perry, D.S., Fraser, G.T., Pine, A.S., 1997. Sub-Doppler infrared spectra and torsion–rotation energy manifold of methanol in the CH-stretch fundamental region. J. Mol. Spectrosc. 185, 158–172.

Yamashita, I., 1975. Crossed-beam experiment on rotational population distribution of OH ($A^2\Sigma^+$) split from H_2O by Lyman alpha photon impact. J. Phys. Soc. Jpn. 39, 205–212.

Ziurys, L.M., Savage, C., Brewster, M.A., Apponi, A.J., Pesch, T.C., Wyckoff, S., 1999. Cyanide chemistry in Comet Hale–Bopp (C/1995 O1). Astrophys. J. 527, L67–L71.